

1 **Running title: *CGR2* and *CGR3* Alters Photosynthesis, and Plant Growth**

2

3 **Co-corresponding authors:**

4 Thomas David Sharkey, Michigan State University, 603 Wilson Rd., 201 Biochemistry, East
5 Lansing, MI, 48824, USA.

6 Phone: (517) 353-6767

7 Fax: (517) 353-9334

8 Email: tsharkey@msu.edu

9

10 Federica Brandizzi, Department of Energy, Plant Research Laboratory, Michigan State
11 University, East Lansing, MI, 48824, USA

12 Phone: (517) 353-7872

13 Fax: (517) 353-1926

14 Email: fb@msu.edu

15

16

17

18

19 **Research area: Biochemistry and Metabolism**

20

21

22 **Pectin Methylesterification Impacts the Relationship Between Photosynthesis and Plant**
23 **Growth in *Arabidopsis thaliana***

24

25 Sarathi Maheshika Weraduwege^{1,2}, Sang-Jin Kim^{2,3,4}, Luciana Renna^{2,3}, Fransisca Chidinma
26 Anozie¹, Thomas David Sharkey^{1,2}, Federica Brandizzi^{2,3,4}

27

28 ¹ Department of Biochemistry and Molecular Biology, Michigan State University, East Lansing,
29 MI 48824, USA

30 ² Department of Energy Plant Research Laboratory, Michigan State University, East Lansing, MI
31 48824, USA

32 ³ DOE Great Lakes Bioenergy Research Center, Michigan State University, East Lansing, MI
33 48824, USA

34 ⁴ Department of Plant Biology, Michigan State University, East Lansing, MI, 48824, USA.

35

36 High levels of methylesterification of pectin allow for enhanced cell expansion, partitioning of
37 resources to leaf growth and increased leaf area for photosynthesis, which in turn enhance plant
38 growth

39

40 Funding for this research was provided by the Chemical Sciences, Geosciences and Biosciences
41 Division, Office of Basic Energy Sciences, Office of Science, U. S. Department of Energy
42 (award number DE-FG02-91ER20021 and in part by the DOE Great Lakes Bioenergy Research
43 Center (DOE Office of Science BER DE---FC02---07ER64494). Partial salary support for TDS
44 and FB came from Michigan AgBioResearch.

45 S.M.W. carried out much of the research, analyzed the data and wrote the manuscript, S.-J.K.
46 and L.R. characterized the mutants and performed cell wall component analysis and part of
47 anatomical studies. F.C.A. provided technical help, S.M.W. and T.D.S and F.B. conceived the
48 experiments and T.D.S and F.B. supervised the research and edited the manuscript.

49

50 **Co-corresponding authors:** Thomas D. Sharkey, tsharkey@msu.edu and Federica Brandizzi,
51 fb@msu.edu

52 **Abstract**

53 Photosynthesis occurs in mesophyll cells of specialized organs such as leaves. The rigid cell wall
54 encapsulating photosynthetic cells controls the expansion and distribution of cells within
55 photosynthetic tissues. The relationship between photosynthesis and plant growth is affected by
56 leaf area. However, the underlying genetic mechanisms affecting carbon partitioning to different
57 aspects of leaf growth is not known. To fill this gap, we analyzed *Arabidopsis thaliana* plants
58 with altered levels of pectin methylesterification, which is known to modulate cell wall plasticity
59 and plant growth. Pectin methylesterification levels were varied through manipulation of *cotton*
60 *Golgi-related (CGR) 2 or 3* genes encoding two functionally redundant pectin
61 methyltransferases. Increased levels of methylesterification in a line overexpressing *CGR2*
62 (*CGR2OX*) resulted in highly expanded leaves with enhanced intercellular air spaces; reduced
63 methylesterification in a mutant lacking both *CGR*-genes (*cgr2/3*) resulted in thin but dense leaf
64 mesophyll that limited CO₂ diffusion to chloroplasts. Leaf, root, and plant dry weight were
65 enhanced in *CGR2OX* but decreased in *cgr2/3*. Differences in growth between wild type and the
66 *CGR*-mutants can be explained by carbon partitioning but not by variations in area-based
67 photosynthesis. Therefore, photosynthesis drives growth through alterations in carbon
68 partitioning to new leaf area growth and leaf mass per unit leaf area (LMA); however, *CGR*-
69 mediated pectin methylesterification acts as a primary factor in this relationship through
70 modulation of the expansion and positioning of the cells in leaves, which in turn drive carbon
71 partitioning by generating dynamic carbon demands in leaf area growth and LMA.

72 **INTRODUCTION**

73 Photosynthesis is the major source of carbon (C) for plant growth. However, there is no clear
74 correlation between area-based photosynthesis and plant growth and studies have shown that the
75 relationship between photosynthesis and plant growth is affected by leaf area growth parameters.
76 A strong positive correlation exists between relative growth rate and leaf growth parameters such
77 as leaf area per unit leaf mass (specific leaf area - SLA), leaf area per unit plant mass (leaf area
78 ratio), and investment of C in leaf growth (leaf mass ratio) (Shipley, 2002; Lambers et al., 2008;
79 Poorter et al., 2009). In fact, modeled partitioning coefficients obtained from the *Arabidopsis*
80 Leaf Area Growth Model showed that plant growth is more sensitive to changes in C partitioning
81 to leaf ‘thickening’ and leaf area growth than to changes to area-based photosynthesis
82 (Weraduwege et al., 2015). The term ‘thickening’ was used to indicate increased mass per unit
83 leaf area (LMA) whether that results from increased thickness in the normal sense of more depth
84 to the leaf between adaxial and abaxial surfaces or from increased cell density. LMA is the
85 reciprocal of SLA. While LMA has been shown to positively and linearly correlate with
86 investment to leaves in the form of anatomical and chemical composition changes, SLA shows a
87 hyperbolic relationship with such changes (Poorter et al., 2009). Therefore, we will mainly focus
88 on LMA throughout this work. Weraduwege et al. (2015) concluded that even though
89 photosynthetic C is required for growth, the degree of growth is determined by the amount of C
90 partitioned to leaf area growth and LMA (Weraduwege et al., 2015). However, how and to what
91 degree this variation in leaf expansion and LMA is affected by cell wall properties of leaf
92 mesophyll cells is not known. In addition, the underlying mechanisms that drive C partitioning to
93 favor either leaf area growth or LMA, and the genes that can influence changes in C demands
94 towards these two processes are yet to be found.

95
96 Leaves are the major photosynthetic organs in plants and regulation of cell expansion and growth
97 is crucial for the development of leaf architecture. Leaf growth can occur in the form of leaf area
98 or LMA (Lambers et al., 2008; Weraduwege et al., 2015). The size and shape of cells in the leaf
99 mesophyll can have a significant impact on: (1) projected or effective leaf surface area, which is
100 the leaf area capable of intercepting light, (2) leaf mass per unit leaf area or LMA, (3) CO₂
101 conductance from the external environment through intercellular air spaces into chloroplasts in
102 mesophyll cells, and (4) on the surface area of mesophyll cells and chloroplasts exposed to

103 intercellular airspaces (Honda and Fisher, 1978; Evans et al., 1994; Galmés et al., 2013). The
104 plant cell wall controls expansion and positioning of cells of photosynthetic tissues and therefore,
105 changes in cell wall properties will have a direct impact on above properties. Although there is
106 evidence for changes in leaf architecture as a result of alterations in genes that affect in synthesis
107 and properties of the cell wall (Burton et al., 2000; Kim and Delaney, 2002; Pilling et al., 2004;
108 Wolf et al., 2009; Kim et al., 2015), an in-depth analysis of affects on leaf gas exchange and
109 overall plant growth under such circumstances has not yet been conducted.

110

111 The plant cell wall is composed mainly of polysaccharides, and among these, pectin is
112 considered a critical element that controls cell wall elasticity and expansion. Pectin is
113 synthesized in the Golgi apparatus and secreted as a highly methylesterified form. In the cell wall
114 the levels of pectin methylesterification vary and are controlled by methyltransferases and
115 methylesterases, which catalyze methylation and demethylation of galacturonic acid in the pectin
116 backbone (Wolf et al., 2009; Kim et al., 2015). Removal of methyl groups allows carboxyl
117 groups of galacturonic acid to form Ca^{2+} and Mg^{2+} -mediated intermolecular linkages that lead to
118 hardening of pectin (Burton et al., 2000; Heldt and Piechulla, 2010; Kim et al., 2015). Indeed,
119 overexpression of pectin methylesterase inhibitors results in longer root cells (Lionetti et al.,
120 2007). Therefore, the degree of methylation and de-methylation of pectin determines the delicate
121 balance between cell wall extensibility and rigidity with consequent effects on growth and shape
122 of cells (Burton et al., 2000; Pilling et al., 2004; Lionetti et al., 2007; Wolf et al., 2009; Xiao and
123 Anderson, 2013; Kim et al., 2015). Consistent with this notion, over-expression of pectin
124 methyltransferases, *CGR2* or *CGR3*, led to enhanced rosette size and fresh weight in *Arabidopsis*
125 (Kim et al., 2015). However, a double knockout of *CGR2* and *CGR3* genes, that was named
126 *cgr2/3*, showed reduced cell expansion and overall plant growth; both phenotypes correlated
127 with reduced levels of pectin methylesterification compared to wild type (Kim et al., 2015). To
128 our knowledge, the effect of pectin methylation on leaf growth parameters, photosynthesis and
129 respiration through its effect on leaf architecture has not been studied.

130

131 The goal of this study was to use the *Arabidopsis* model system developed by Kim et al. (2015)
132 with altered levels of pectin methyltransferases, *CGR2* or *CGR3*, which are single gene modifiers
133 found to positively or negatively affect cell expansion in function of their cellular availability, to

134 investigate how changes in cell wall plasticity affect C assimilation, leaf respiration and overall
135 plant growth through effects on leaf area growth and mesophyll structure. We examined whether
136 the changes in overall plant growth in *Arabidopsis* with altered *CGR2* and *CGR3* could result
137 from changes in leaf area growth and LMA or changes in area-based photosynthesis to explore
138 the relationship between photosynthesis and growth. Based on the differences in rosette size
139 reported previously (Kim et al., 2015), we hypothesized that area-based photosynthesis rates
140 would be lower in a *CGR2* overexpressor (*CGR2OX*) but larger in *cgr2/3*. As *CGR2* and *CGR3*
141 affect pectin methylation and cell expansion in leaves, we also hypothesized that plant growth
142 would be enhanced in the *CGR2OX* line and reduced in the *cgr2/3* mutant mainly as a result of
143 altered LMA. Indeed, through analysis of leaf and plant growth, gas exchange, and growth
144 modelling, we found that *CGR2* and *CGR3* have significant impacts on photosynthesis and
145 respiration through alteration of mesophyll structure and LMA. Plant growth was enhanced in
146 the *CGR2OX* line but reduced in the *cgr2/3* mutant. This variation in plant growth was as a
147 result of differences in C partitioning and not as a result of changes in photosynthetic rate per
148 unit leaf area. These observations support a novel model that changes in cell wall plasticity due
149 to changes in pectin composition influences C partitioning between leaf area growth and LMA
150 thereby regulating the relationship between photosynthesis and plant growth.

151

152 **MATERIALS AND METHODS**

153 **Growth Analysis**

154 Wild type *Arabidopsis thaliana* (Col-0), *cgr2/3* (loss of function double mutant line of *CGR2*
155 and *CGR3*), *CGR2OX* (*CGR2* overexpression line), and *cgr2com* (*cgr2/3* complemented by
156 *CGR2*) (Kim et al., 2015) were used in the study. Gene accession numbers for *CGR2* and *CGR3*
157 are At3g49720 and At5g65810, respectively. Plants were grown hydroponically in ½ strength
158 Hoagland's solution, under a light intensity of 120 $\mu\text{mol m}^{-2} \text{s}^{-1}$ and an 8 h photoperiod, daytime
159 and nighttime temperature of 22°C and 20°C respectively, and 60% relative humidity. The
160 hydroponics system was housed in a GC-20, Bigfoot series growth chamber (BioChambers Inc.,
161 Winnipeg, MB, Canada).

162

163 Plant growth parameters including projected and total leaf area, leaf, root, and inflorescence dry
164 weights, relative growth rates, SLA, LMA, leaf area ratio, and leaf, root, and inflorescence mass

165 ratios were measured as described in Weraduwege et al. (2015). When calculating SLA, LMA,
166 leaf area ratio, and leaf, root, and inflorescence mass ratios, the total leaf area, and organ and
167 plant mass corresponding to each harvest was used: SLA ($\text{m}^2 \text{kg}^{-1}$) = total leaf area/leaf mass;
168 LMA (kg m^{-2}) = leaf mass/total leaf area; leaf area ratio (g g^{-1}) = total leaf area/total plant mass;
169 leaf, root or inflorescence mass ratio (g g^{-1}) = leaf, root or inflorescence mass/total plant mass.
170 Growth measurements were obtained throughout the life cycle of the plant at 2-3 week intervals
171 at 29, 49, 63, and 82 days after seeding (DAS). The 100-seed weight prior to stratification and
172 sowing, cotyledon area and hypocotyl length was also measured.

173

174 **Determination of Leaf Thickness, Mesophyll Cell Density, S_{mes} , S_{c} , and Chloroplast Size** 175 **and Abundance**

176 Leaves of similar age from 34 and 51 day old rosettes were used for anatomical measurements.
177 Leaves were harvested and processed for leaf cross-sectioning as described in Weraduwege et
178 al., 2015, at the Center for Advanced Microscopy, Michigan State University. Thin (500 nm) leaf
179 sections (PTXL ultramicrotome, RMC, Boeckeler Instruments, Tucson, AZ) were observed
180 under an Olympus SpectralView FV1000, Confocal Laser Scanning Microscope (Olympus, NJ,
181 USA) and the distance between the adaxial and abaxial leaf surfaces was measured to determine
182 leaf thickness.

183

184 Micrographs of leaf cross sections were used to determine the number of palisade and spongy
185 parenchyma cells, the total number of cells, and the number of mesophyll cell layers in a 20,000
186 μm^2 area of a leaf cross section. This data was later expressed per mm^2 . ImageJ (<http://imagej.nih.gov/ij/>) software was utilized to measure the total area of intercellular air spaces, total length
187 of mesophyll cells, total length of mesophyll cells exposed to intercellular air spaces (L_{mes}), and
188 the total length of chloroplasts exposed to intercellular air spaces (L_{c}). The latter three
189 measurements were utilized to determine the surface area of mesophyll cells exposed to
190 intercellular air spaces (S_{mes}) and the surface area of chloroplast exposed to intercellular air
191 spaces (S_{c}) per unit leaf area as described in Evans et al. (1994).

193

194 A series of z-stack images of leaves of 34 day old plants was acquired using an inverted laser
195 scanning confocal microscope (Zeiss LSM510 META, <http://www.zeiss.com>). Chloroplasts were

196 imaged using an ECPlan-Neofluar 40X/1.30 oil M27 objective at a 512x512 pixel resolution
197 using an excitation wavelength of 514 nm and an emission wavelength of 673 nm. The different
198 planes acquired were then projected on the same image and transformed in binary using Image J.
199 The resulting number of chloroplasts per unit area and average chloroplast size was measured
200 using ImageJ software.

201

202 **Gas Exchange Measurements, $^{14}\text{CO}_2$ Feeding Experiments, and Analysis of Leaf ^{13}C**

203 **Discrimination**

204 Whole rosette photosynthesis and nighttime dark respiration was measured at 2-3 week intervals
205 at 29, 49, 63, 82 days after seeding (DAS). A custom-built rosette-gas-exchange chamber
206 connected to a LI-COR 6400 portable gas exchange system (LI-COR Biosciences, Inc., Lincoln,
207 NE) was used to obtain photosynthesis and respiratory measurements. Conditions in the
208 *Arabidopsis* rosette gas-exchange chamber during photosynthesis measurements were: a leaf
209 temperature of 22°C, $[\text{CO}_2]$ of 400 ppm, $120 \mu\text{mol m}^{-2} \text{s}^{-1}$ light intensity. During nighttime
210 respiration measurements the leaf temperature was maintained at 20°C. Flow rate was set at 500
211 $\mu\text{mol s}^{-1}$ when making measurements from 49 and 63 day old plants. For 29 and 82 day old
212 plants, flow rate was set at 300, and 700 $\mu\text{mol s}^{-1}$, respectively in order to better control
213 humidity.

214

215 After the initial measurements of photosynthesis, 29 day old *Arabidopsis* rosettes were fed with
216 $^{14}\text{CO}_2$ for 10 minutes. After a 2 h chase period, leaf and root tissue were harvested separately
217 into scintillation vials. Radioactivity was determined as disintegrations per minute (DPM) by
218 liquid scintillation counting. The DPM recorded from roots and rosettes and the total DPM was
219 used to calculate the proportion of C present in these organs.

220

221 The content ratio of $^{13}\text{CO}_2$ to $^{12}\text{CO}_2$ in *Arabidopsis* freeze-dried leaf material was measured at the
222 Stable Isotope Ratio Facility for Environmental Research, University of Utah by mass
223 spectrometry. This data was used to calculate the $\delta^{13}\text{C}_{\text{VPDB}}$ value which is the ^{13}C to ^{12}C isotopic
224 ratio of leaves relative to the ^{13}C to ^{12}C isotopic ratio of the Vienna-Pee-Dee Belemnite (VPDB)
225 standard (Farquhar et al., 1982). The $\delta^{13}\text{C}_{\text{VPDB}}$ values were used to calculate the CO_2 partial
226 pressure at rubisco using equation 12 given in Farquhar et al. (1982). Values for the various

227 factors are as follows: δ value of CO₂ in the air at present = - 8.4‰ (<http://www.esrl.noaa.gov>),
228 partial pressure of CO₂ in the air = 39 Pa, ¹³C discrimination associated with the diffusion of CO₂
229 through air = 4.4‰, ¹³C discrimination in the carboxylation reaction = 27‰ (Farquhar et al.,
230 1989).

231

232 **Analysis of Cell Wall Polysaccharides in Leaves**

233 Preparation of alcohol-insoluble residues (AIR), uronic acid assays and methyl ester assays were
234 performed based on the methodology described in Kim et al. (2015). The matrix polysaccharide
235 (hemicellulose) and crystalline cellulose composition, and soluble sugar content in leaves were
236 measured at the Great Lakes Bioenergy Research Center Cell-Wall Facility, Michigan State
237 University (East Lansing, MI) as described in Kim et al. (2015).

238

239 **Parameterization of the *Arabidopsis* Leaf Area Growth Model**

240 Development, parameterization and execution of the *Arabidopsis* Leaf Area Growth Model were
241 described in detail in Weraduwege et al. (2015). This model is a tool to determine partitioning
242 coefficients of C that could give rise to the growth patterns observed in different plants
243 (Weraduwege et al., 2015). In the model, plant growth is divided into four growth stages: (1)
244 heterotrophic phase (1-4 DAS), (2) early vegetative phase, (3) late vegetative phase, and the (4)
245 reproductive phase. Ninety days of plant growth is simulated in the model using a fixed time step
246 of 1 h and the photoperiod is set at 8 h. As described in detail in Weraduwege et al. (2015), the
247 following was used as inputs of the model: weight of storage reserves, ratio of mobilized storage
248 reserves to stored reserves, initial leaf area, initial leaf mass, projected to total leaf area ratio, net
249 photosynthesis rate per unit leaf area, proportion of C stored as starch during the day, leaf
250 maintenance and growth respiratory coefficients, photoperiod, lengths of growth phases.

251

252 Values for area-based photosynthesis obtained during the four harvests were fitted with a
253 polynomial 3rd order equation to extrapolate area-based photosynthesis through the entire 90
254 days of the life cycle. Similarly, measured projected to total leaf area ratios during the four
255 harvests was fitted with a polynomial 2nd order equation to extrapolate the values over 90 days.
256 These extrapolated values were used in the model as input photosynthesis values and projected to
257 total leaf area ratios over the life span. The model also takes both growth and maintenance

258 respiration into consideration. The model considers maintenance respiration of a plant/particular
259 organ to be proportional to the corresponding dry mass and growth respiration to be proportional
260 to the growth rate (De Vries et al., 1974; Amthor, 1984; Thomas et al., 1993; Lambers et al.,
261 2008). The model has set values for maintenance coefficients (amount of C respired to maintain
262 the existing mass of the plant or specific organ, $\mu\text{mol C g}^{-1} \text{ s}^{-1}$), and for growth coefficients
263 (amount of C respired per unit increase in mass, g g^{-1}) based on values provided in the literature
264 (Amthor, 1984; Mariko, 1988) and assumes that growth respiration coefficients of leaf growth in
265 terms of area and LMA are the same throughout the life cycle. The net amount of C available for
266 growth and maintenance processes of the plant is determined as the product of area-based
267 photosynthetic rate and the projected leaf area. Next, C consumed in maintenance respiration and
268 exudation is subtracted to determine the net assimilation rate, which provides the amount of C
269 available for growth. The model then simulates the partitioning of C available for growth to leaf
270 area growth, growth in terms of LMA, and root and inflorescence growth based on the set
271 partitioning coefficients which are adjustable to facilitate fitting of the data. Partitioning
272 coefficients vary based on the growth phases. The increase in mass during growth in terms of
273 leaf area and LMA, and root and inflorescence growth is calculated by subtracting the C
274 consumed in growth respiration from the total C allocated for growth of that particular organ.
275 Accordingly, the model simulates the increase in leaf area and mass, and the mass of the
276 inflorescence and roots. The model calculated SLA, LMA, and leaf, root and inflorescence mass
277 ratios over time based on the equations given above.

278 In order to fit the modeled data to measured data, 16 partitioning coefficient parameters
279 (partitioning to the inflorescence, roots, leaf area and LMA, for each of the four growth phases:
280 germination phase, early and late vegetative phases, and reproductive phase), were adjusted so
281 that the modeled and measured leaf area, mass of inflorescence, root, and leaf matched
282 (Weraduwage et al., 2015). C partitioning data obtained by feeding *Arabidopsis* rosettes at 29
283 DAS with $^{14}\text{CO}_2$ were used as initial estimates which were fine tuned to fit the data. Sensitivity
284 of the model to changes in the inputs was tested in Col-0 by simulating an increase or decrease of
285 1% in C partitioned to growth processes, and other model inputs, and noting the resulting
286 response in output. The model was considered sensitive, in cases where more than 1% variation
287 occurred in model outputs as a consequence of changing a particular input.

288 **Statistical Analyses of Experimental Data**

289 Four to five biological replicates per line were used to collect experimental data at a given time
290 point. Statistical analyses were carried out using SPSS 22 (IBM Corporation, NY, NY). The
291 effects of altered *CGR2* and *CGR3* expression on plant growth and gas exchange were compared
292 using a univariate general linear model and the differences between means were tested by
293 subjecting data to one-way ANOVA at $\alpha = 0.05$, followed by a Least Significant Difference Test.
294 Measured data presented in figures represent the mean \pm standard error (SE).

295

296 **RESULTS**

297 **CGR2OX and *cgr2/3* Mutant Lines Retained Altered Cell Wall Composition**

298 Cell wall composition of Col-0, *cgr2com*, CGR2OX and *cgr2/3* was analyzed in order to
299 determine whether the previously observed changes in methylesterification and modification of
300 cell-wall polysaccharides by Kim et al. (2015) was retained in the mutant lines. Similar to what
301 was seen by Kim et al. (2015), crystalline cellulose content was lower in *cgr2/3* mutant line and
302 it was greater in CGR2OX than that in Col-0 (**Supplemental Fig. S1A**). In addition, neutral
303 sugars such as fucose, arabinose, and glucose content was significantly higher in *cgr2/3* than
304 Col-0 as was shown by Kim et al. 2015 (**Supplemental Fig. S1B**). The uronic acid content and
305 the amount of methylesters per uronic acid were greater in CGR2OX compared to wild type
306 (Col-0); the uronic acid content was lower in *cgr2/3* (**Supplemental Fig. S1C-D**). These data
307 support that the cell wall composition, including pectin and the degree of methylesterification is
308 altered in the CGR2OX and *cgr2/3* mutant lines in response to altered *CGR2* and *CGR3* gene
309 expression, as previously reported (Kim et al., 2015).

310

311 **Enhanced Pectin Methylesterification Increases Leaf Area while a Decrease in Pectin**
312 **Methylesterification Reduces Leaf Area.**

313 Hypocotyl length, and cotyledon and leaf areas were measured in order determine how altered
314 expression of *CGR2* and *CGR3* affects early seedling growth, and expansion of the leaf blade.
315 Similar to earlier results (Kim et al., 2015), hypocotyls of CGR2OX were significantly longer
316 than wild type (Col-0), while those of *cgr2/3* were shorter (**Supplemental Figs. S2A and S3A**).
317 Cotyledon area was also smaller in *cgr2/3* than Col-0 (**Supplemental Fig. S3A**). The CGR2OX
318 mutant produced rosettes with greater projected and total leaf area compared to Col-0 throughout

319 the life cycle (**Fig. 1, Supplemental Fig. S2, B and C**). In contrast, a significant reduction in
320 projected and total leaf area was observed in *cgr2/3*. The degree of leaf overlap measured by the
321 ratio between projected and total leaf area was not different between the transgenic lines and
322 Col-0 (**Figure 1**). Thus, functional availability of *CGR2* and *CGR3* has a significant impact on
323 leaf area growth.

324

325 **Genetic Depletion of *CGR2* and *CGR3* Results in Thin Leaves with Small, Densely Packed** 326 **Mesophyll Cells**

327 Leaf area and thickness are generally negatively correlated (Lambers et al., 2008; Weraduwage
328 et al., 2015). In order to determine whether changes in leaf area in *CGR2OX* and *cgr2/3* were
329 accompanied by changes in leaf thickness, we measured leaf thickness. Interestingly, leaves of
330 *cgr2/3* were both thin and of small leaf area (**Fig. 2, A and B**); this trend was observed
331 throughout the life cycle (data not shown). During early vegetative growth (34 DAS), *CGR2OX*
332 produced thinner leaves with a tendency toward more area than Col-0. Nonetheless, the
333 *CGR2OX* leaves were thicker than those of *cgr2/3*.

334

335 Next, we determined whether *CGR2* and *CGR*- mediated pectin methylesterification was
336 correlated with changes in mesophyll architecture. *CGR2OX* had larger palisade cells and 3-4
337 mesophyll cell layers compared to Col-0, which produced 4-5 layers of comparatively smaller
338 palisade cells (**Fig. 2A**). However, the mesophyll cells of *cgr2/3* were significantly smaller and
339 more numerous than in Col-0 (**Fig. 2A**) which lead to a marked reduction in intercellular
340 airspaces in the leaf mesophyll (**Fig. 2C**). Consequently, a significant negative correlation was
341 observed between the number of cells and intercellular air spaces in the leaf mesophyll (**Fig.**
342 **2C**). Enhanced cell density and the reduction in intercellular air spaces in *cgr2/3* compared to the
343 other *Arabidopsis* lines also led to a significant reduction in mesophyll cell surface area (S_{mes})
344 and chloroplast surface area (S_c) exposed to intercellular air spaces per unit leaf area (**Fig. 2, D**
345 **and E**).

346

347 Interestingly also, the number of chloroplasts per unit area of a leaf cross section was lower in
348 *CGR2OX* and greater in *cgr2/3* compared to Col-0 (**Fig. 3A**). However, the average size of
349 chloroplasts was smaller in all transgenic lines compared to Col-0 (**Fig. 3B**). The data indicate

350 that the reduction in S_c in *cgr2/3* was not as a result of a reduction in chloroplast area per unit
351 leaf area, but was linked to the significant reduction in intercellular air spaces in the leaf
352 mesophyll. Therefore, our results show that variations in the levels of methylesterification of the
353 cell wall significantly impact leaf thickness, cell density, and mesophyll architecture.

354

355 **Changes in Mesophyll Architecture due to Alterations in *CGR*-Expression Affects Area-** 356 **Based Photosynthesis and Respiration**

357 We next aimed to establish whether changes in mesophyll architecture as well as projected and
358 total leaf areas affect net C assimilation in mutant lines with altered *CGR*-expression. To do so,
359 we measured area- and plant-based photosynthesis and respiration. During early vegetative
360 growth, at around 29 DAS, area-based photosynthesis in *cgr2/3* was significantly higher than the
361 other lines (**Fig. 4A**). Afterwards, *cgr2/3* showed lower area-based photosynthesis rates
362 compared to Col-0 throughout the vegetative growth phase (**Fig. 4A**). Area-based photosynthesis
363 in CGR2OX was lower than Col-0 around 49 DAS, but, remained higher compared to *cgr2/3*.
364 We also established that area-based respiration in *cgr2/3* was 2-5 times greater than Col-0 (**Fig.**
365 **4B**). Thus, photosynthesis to respiration ratio remained significantly smaller in *cgr2/3*
366 throughout the life cycle (**Fig. 5A**). Although, not statistically significant at the 5% level,
367 CGR2OX showed a trend towards lower area-based respiration (**Fig. 4B**) and therefore, its
368 photosynthesis to respiration ratio appeared to be greater in young rosette leaves at 29 DAS (**Fig.**
369 **5A**). Increased area-based respiration in *cgr2/3* and lower area-based respiration in CGR2OX,
370 correlated well with the differences in the number of mesophyll cells in these lines (**Fig. 2C**). In
371 general, plant-based photosynthesis in CGR2OX was similar to Col-0 with an upward trend,
372 even though, area-based photosynthesis was smaller (**Fig. 4, A and C**); this was mainly due to
373 the larger projected leaf area in CGR2OX (**Fig. 1A**). However, owing to its smaller projected
374 leaf area, plant-based photosynthesis in *cgr2/3* was much lower than Col-0 (**Fig. 4C**). Plant-
375 based respiration was greater in CGR2OX, and smaller in *cgr2/3* than in Col-0 (**Fig. 4D**), which
376 could be explained by differences in total leaf area (**Fig. 1B**).

377

378 Daily C gain in rosettes was greater in CGR2OX compared to Col-0 when measured at 29 and 49
379 DAS, while it was significantly smaller in *cgr2/3* (**Fig. 5B**). The upward trend in daily C gain
380 observed in CGR2OX was a result of its higher plant-based photosynthetic rates due to greater

381 projected leaf area (**Figs. 1A and 4C**). The decrease in C gain in *cgr2/3* resulted from reduced
382 plant-based photosynthesis due to the smaller projected leaf area and smaller photosynthesis:
383 respiration ratio compared to CGR2OX (**Figs. 1A, 4C and 5A**). Together these results support
384 the hypothesis that by controlling leaf area and mesophyll architecture, pectin
385 methylesterification is a critical factor for regulation of whole plant rates of photosynthesis and
386 respiration.

387

388 **Suppression of Pectin Methylesterification Leads to a Reduction in CO₂ Availability for** 389 **Photosynthesis**

390 The differences in chloroplast number and size could not account for the large differences
391 observed in area-based photosynthesis between *cgr2/3* and the other three *Arabidopsis* lines (**Fig.**
392 **3, A and B**). Therefore, in order to investigate whether lower area-based photosynthesis in
393 *cgr2/3* at harvests 2, 3, and 4 was a result of a reduction in CO₂ availability owing to altered
394 mesophyll architecture, the degree of ¹³C discrimination was analyzed in leaf tissue of the four
395 *Arabidopsis* lines. The ¹³C content of *cgr2/3* was greater consistent with less discrimination
396 against ¹³CO₂ during photosynthesis compared to the other lines (**Fig. 6, A-C**). The average CO₂
397 partial pressure at rubisco calculated using the $\delta^{13}\text{C}_{\text{VPDB}}$ values showed CO₂ availability to be
398 significantly lower in *cgr2/3* (**Fig. 6, D-F**). These data are in agreement with the hypothesis that
399 there is a greater resistance to CO₂ diffusion into chloroplasts of *cgr2/3* owing to lower surface
400 areas of mesophyll cells and chloroplasts facing intercellular air spaces per unit leaf area as a
401 result of enhanced cell density and reduced intercellular air spaces (**Fig. 2, C-D**). Therefore,
402 reduction in *CGR2* and *CGR3* availability appears to have a strong negative impact on area-
403 based photosynthesis owing to reduction in CO₂ availability to chloroplasts, most likely as a
404 result of altered mesophyll architecture.

405

406 **A Decrease in Pectin Methylesterification Increased LMA, and Reduced Plant Growth and** 407 **Relative Growth Rates.**

408 We next analyzed the effects of altered expression of *CGR2* and *CGR3* on plant growth by
409 measuring leaf growth parameters, plant biomass, and relative growth rates. We found that LMA
410 was higher in *cgr2/3* during the early to late vegetative phases around 29 to 63 DAS (**Fig. 7A**). In
411 addition, LMA in CGR2OX remained significantly lower than in *cgr2/3*. Leaf area per unit plant

412 mass (leaf area ratio) and leaf mass ratio (mass of leaf per unit plant mass) were significantly
413 smaller in *cgr2/3* than other lines (**Fig. 7, B and C**). In contrast, root mass ratio (mass of root per
414 unit plant mass) was larger in *cgr2/3* than other lines (**Fig. 7D**).

415
416 Interestingly, *CGR2OX* maintained the greatest leaf, root and plant biomass throughout the life
417 cycle (**Fig. 8, A-D**). In contrast, *cgr2/3* plants exhibited a significant reduction in leaf, root and
418 plant dry weight throughout the life cycle. Collectively, these data reveal that alterations in
419 *CGR2* and *CGR3* expression can have a significant effect not only on leaf growth, but also on
420 overall plant growth. Therefore, while an increase in pectin methylesterification enhances plant
421 biomass, a decrease in pectin methylesterification reduces it. Modeled relative growth rates
422 revealed that both area-based (**Fig. 9A**) and mass-based (**Fig. 9B**) relative growth rates were
423 higher in *CGR2OX* and smaller in *cgr2/3* than Col-0 during most part of the life cycle. In
424 summary, alterations in *CGR2* and *CGR3* has a significant impact on important leaf growth
425 parameters such as LMA, and biomass partitioning to leaf growth, and also affects plant growth
426 in terms of biomass accumulation and relative growth rates. LMA showed a negative correlation
427 with plant growth and relative growth rates.

428

429 **Enhanced Pectin Methylesterification and C Partitioning to Leaf Area Growth**

430 The *Arabidopsis* Leaf Area Growth Model parameterized with measurements obtained from the
431 four *Arabidopsis* lines was used to estimate how much C was partitioned to new leaf area growth
432 and LMA, as a proportion of net assimilated C that is available for growth. These values,
433 referred to as partitioning coefficients (**Table 1**), would allow determination of whether changes
434 in *CGR2* and *CGR3* availability could affect C partitioning to growth or respiratory processes.
435 The proportions of C partitioned to leaf growth in total (C partitioned to area + LMA), and to
436 root growth found by $^{14}\text{CO}_2$ feeding experiments at 29 DAS were used as an initial estimate
437 when setting the partitioning coefficients to leaf growth for the early vegetative growth phase
438 (**Supplemental Fig. S4, Table 1**). Partition coefficients obtained from growth modelling for
439 *CGR2OX* revealed that, compared to the other lines, the overexpression line of *CGR2* partitioned
440 more of the C available for leaf growth towards leaf area growth and less towards LMA,
441 especially during the early vegetative phase (**Table 1**). In contrast, we found that in *cgr2/3* a
442 significantly greater proportion of C was allocated to LMA rather than to leaf area growth

443 (Table 1). The differences in C partitioning to leaf area growth and LMA between Col-0 and
444 CGR2OX and *cgr2/3* were most prominent during early vegetative phases of growth.

445
446 The patterns of C partitioning in transgenic lines seen in Table 1 were further investigated by
447 determining the amounts of C being partitioned to specific growth processes as well as
448 respiratory processes as a proportion of the total available C in the plant (Fig. 10). CGR2OX,
449 still partitioned a greater proportion of total available C to leaf area growth and a lesser
450 proportion to LMA compared to the other lines; *cgr2/3* showed an opposite trend to that seen in
451 CGR2OX (Fig. 10). The maintenance respiratory cost increased as the plant aged. Towards the
452 end of its life cycle (82 DAS), close to 75% of assimilated C was consumed in maintenance
453 respiration (Fig. 10). While the maintenance costs in CGR2OX was somewhat larger than Col-0
454 towards the end of the life cycle, a significant enhancement in the proportion of C spent in
455 maintenance respiration could be seen in *cgr2/3* throughout the life cycle (Fig. 10). Collectively,
456 data provide evidence to support that alteration in *CGR2* and *CGR3* expression has a significant
457 impact on determining the proportions of C partitioned to new leaf area growth versus LMA, and
458 to maintenance respiration in plants.

459 460 **Growth in CGR2OX and *cgr2/3* is Affected More by Alterations in C Partitioning than by** 461 **Changes in Area-based Photosynthesis**

462 In order to determine whether the alterations in growth observed in CGR2OX and *cgr2/3* were a
463 result of alterations in area-based photosynthesis (Fig. 4A) or partitioning coefficients to leaf
464 area growth and LMA growth (Table 1), the values for these parameters in the growth model for
465 Col-0 were substituted separately by corresponding values from the two transgenic lines.
466 Interestingly, by keeping the partitioning coefficients the same, substitution of area-based
467 photosynthesis rates for 1-90 days with those of CGR2OX resulted in a small reduction in
468 modeled growth in Col-0 whereas *cgr2/3* caused a large increase in growth (gray lines in Fig.
469 11).

470
471
472

473 **Table 1: Comparison of modeled partition coefficients during different growth phases for**
474 ***Arabidopsis* lines with altered pectin methyltransferase expression.** Partitioning coefficients
475 for partitioning of net assimilated C to inflorescence and root growth, LMA, and leaf area growth
476 during the early and late vegetative phases and the reproductive phase for Col-0, *cgr2com*,
477 *CGR2OX*, and *cgr2/3* were obtained from the *Arabidopsis* Leaf Area Growth Model. The
478 durations of the early and late vegetative phases and the reproductive phase for each line is as
479 follows: for Col-0, 5 -51 DAS, 52 - 74 DAS and 75 - 90 DAS; for *cgr2com*, 5 - 48 DAS, 49 - 70
480 DAS and 71 - 90 DAS; for *CGR2OX*, 5 -49 DAS, 50 - 72 DAS and 73 - 90 DAS; for *cgr2/3*,
481 assuming flower initiation started at 82DAS, 5 - 55 DAS, 56 - 81 DAS and 82 - 90 DAS.

<i>Arabidopsis</i> line	Organ/process to which C is partitioned	Partitioning coefficients		
		Early vegetative growth phase	Late vegetative growth phase	Reproductive growth phase
Col-0	Inflorescence growth	0.00	0.02	0.30
	Root growth	0.06	0.13	0.12
	LMA	0.17	0.10	0.10
	Leaf area growth	0.77	0.75	0.48
<i>cgr2com</i>	Inflorescence growth	0.00	0.03	0.40
	Root growth	0.03	0.12	0.12
	LMA	0.19	0.10	0.10
	Leaf area growth	0.78	0.75	0.38
<i>CGR2OX</i>	Inflorescence growth	0.00	0.03	0.30
	Root growth	0.04	0.15	0.15
	LMA	0.16	0.11	0.10
	Leaf area growth	0.80	0.71	0.45
<i>cgr2/3</i>	Inflorescence growth	0.00	0.00	0.10
	Root growth	0.10	0.25	0.25
	LMA	0.24	0.18	0.10
	Leaf area growth	0.66	0.57	0.55

482

483

484 However, by keeping area-based photosynthesis the same, substituting the partitioning
485 coefficients of Col-0 with that of *CGR2OX* had a strikingly large positive effect on modeled
486 growth; *cgr2/3* partitioning coefficients had a significantly large negative effect on growth which
487 mirrored the observed differences in growth in the *CGR2* overexpression line and the *CGR2* and
488 *CGR3* double mutant lines (orange lines in **Fig. 11**). These observed changes in growth could be
489 achieved by substituting the partitioning coefficients of only the early vegetative growth phase
490 (data not shown). The data show that the observed changes plant growth in *CGR2OX* and *cgr2/3*
491 were not a result of differences in photosynthetic rates, but a result of differences in C
492 partitioning to growth in terms of leaf area and LMA especially during early vegetative growth.
493 Thus, our data support the hypothesis that the magnitude of plant growth is determined by how
494 photosynthetic carbon is partitioned to new leaf area growth and LMA.

495

496 **DISCUSSION**

497 In this study, we investigated how modification of cell wall plasticity via the genetic
498 manipulation of pectin methyltransferases, *CGR2* and *CGR3*, affects C assimilation, leaf
499 respiration and overall plant growth through effects on leaf area growth and mesophyll structure.
500 We also wanted to further understand the relationship between photosynthesis and plant growth
501 by determining whether the changes in overall plant growth in *Arabidopsis* with altered cellular
502 availability of *CGR2* and *CGR3* were a result of changes in growth in terms of leaf area and
503 LMA or due to changes in area-based photosynthesis. We found that overexpression of *CGR2*
504 has a significant positive effect on leaf area and plant growth. On the other hand, suppression of
505 *CGR2* and *CGR3* expression caused a marked increase in LMA and a reduction in leaf area and
506 plant growth. Altered expression of *CGR2* and *CGR3* also had a significant impact on
507 photosynthesis and respiration through altered mesophyll architecture. The differences in plant
508 growth in *Arabidopsis* with altered *CGR2* and *CGR3* levels were linked to changes in C
509 partitioning to leaf area growth and LMA rather than altered area-based photosynthesis rates.
510 These findings establish that *CGR2* and *CGR3* mediated pectin methylesterification affects
511 mesophyll architecture, C accumulation, C partitioning, leaf and plant growth, and the
512 relationship between photosynthesis and plant growth.

513

514 ***CGR2* and *CGR3* Directly Affect Leaf Mass per Unit Area by Altering Both Leaf Thickness**
515 **and the Mass of Leaf per Unit Volume of Leaf Tissue**

516 Often, thicker leaves are associated with larger LMA due to an increase in the number of cell
517 layers, which can increase leaf mass per unit leaf area (Lambers et al., 2008; Poorter et al., 2009;
518 Villar et al., 2013; Weraduwege et al., 2015). However, a negative correlation exists between
519 leaf mass density or LMD (mass of leaf per unit volume of leaf tissue) and leaf thickness, and
520 both parameters can affect LMA as follows; $LMD (kg\ m^{-3}) = \text{leaf mass} / (\text{leaf area} \times \text{leaf}$
521 $\text{thickness})$; $LMA (kg\ m^{-2}) = LMD \times \text{leaf thickness}$ (Witkowski and Lamont, 1991; Lambers et
522 al., 2008; Poorter et al., 2009; Villar et al., 2013). Therefore, leaf ‘thickening’ or an increase in
523 LMA can occur due to an increase in leaf thickness or LMD. While thicker leaves have been
524 shown to be associated with larger mesophyll cells (elongated, especially in the depth direction)
525 and larger air spaces, LMD has been associated with smaller proportions of intercellular air
526 spaces and smaller cells (Tsuge et al., 1996; Poorter et al., 2009; Villar et al., 2013). In addition
527 to being affected by anatomical changes, LMA and LMD can also be determined by variations in
528 cellular and chemical composition (Cunningham et al., 1999; Lambers et al., 2008). For
529 example, plants with slow growth rates possess a larger number of smaller cells with thicker cell
530 walls, and a greater proportion of lignin and other cell wall polysaccharides per unit leaf area that
531 can increase LMD and LMA (Cunningham et al., 1999; Lambers et al., 2008). A key aspect of
532 cellular mass is formed by organelles and plants with higher growth rates may possess large cells
533 with a lower number of chloroplasts that result in lower LMA (Lambers et al., 2008).

534
535 Interestingly, while both *CGR2OX* and *cgr2/3* had thinner leaves compared to *Col-0*, *cgr2/3*
536 showed a significant increase in LMA. Such increase in *cgr2/3* can be attributed to increased
537 LMD as a result of enhanced cell density and reduction of intercellular air spaces in the leaf
538 mesophyll. Smaller cells can lead to concentration of cellular metabolites, which can also lead to
539 increased LMD. In addition, *cgr2/3* also possessed a larger number of chloroplasts/leaf area. The
540 proportions of cell wall components per unit leaf area are also likely greater in *cgr2/3* compared
541 to the other backgrounds. Therefore, collectively the data clearly show that although *cgr2/3* had
542 thinner leaves, enhanced LMD led to greater leaf mass per unit area (or lower SLA) in *cgr2/3*.
543 Conversely, LMA in *CGR2OX* was significantly smaller than *cgr2/3*. Leaves of *CGR2OX* were
544 also thicker than *cgr2/3* and contained larger intercellular airspaces, and larger cells with a lower

545 number of chloroplasts. Therefore, our results support that variation in LMA between CGR2OX
546 and *cgr2/3* resulted from the combination of increased leaf thickness and reduced leaf mass
547 density.

548
549 The significant alterations in mesophyll architecture observed during the present study are linked
550 to changes in *CGR2* and *CGR3* expression. Based on the model that reduced methylation of
551 pectin may enhance Ca^{2+} mediated cross-linking of galacturonic acid in cell walls thereby
552 preventing normal cell expansion in *cgr2/3* (Burton et al., 2000; Wolf et al., 2009; Kim et al.,
553 2015), we proposed that the larger number of smaller mesophyll cells observed during the
554 present study is likely linked to the hardening of the cell wall and consequent restriction of cell
555 wall expansion. This in turn is likely to cause an increase of cell number/leaf area in *cgr2/3*
556 compared to Col-0. In addition, cross-linking between galacturonic acid and Ca^{2+} in cell wall
557 pectin is required for cellular adhesion (Caffall and Mohnen, 2009). Also a reduction in
558 galacturonic acid- Ca^{2+} complex formation in *Lycopersicon esculentum* resulted in large air
559 spaces in the fruit pericarp caused by dramatic reductions in the middle-lamellae-mediated cell to
560 cell adhesion (Caffall and Mohnen, 2009). The observed decrease in air spaces in *cgr2/3* and the
561 dense distribution of the cells (hence thinner leaves) is likely due to enhanced cell-to-cell
562 adhesion as a result of the lower degree of methylesterified pectin in *cgr2/3* compared to Col-0.
563 In contrast, enhanced methylation of pectin promotes cell expansion (Kim et al. 2015); this
564 resulted in the observed presence of wider palisade cells and a fewer number of cell layers
565 (hence thinner leaves) in CGR2OX than Col-0. The number of cells and area of airspaces in
566 CGR2OX differed only marginally from Col-0. However, CGR2OX did have a smaller number
567 of smaller chloroplasts compared to Col-0, which may be an indication of lower LMA. Whether
568 overexpression of *CGR2* has a dosage effect and whether overexpression of both *CGR2* and
569 *CGR3* would result in larger and thicker leaves with lower cell density remains to be
570 investigated.

571
572 Thinner leaves usually correlate with larger SLA or smaller LMA (Lambers et al., 2008;
573 Weraduwege et al., 2015). However, based on the negative correlation between LMD and leaf
574 thickness, it is likely that LMD would start to increase should leaf thickness decrease below a
575 certain optimum, thereby resulting in an increase in LMA. This was demonstrated in *cgr2/3*,

576 where suppression of *CGR2* and *CGR3* resulted in leaves that were too thin, leading to higher
577 cell density and LMA. This can have significant negative effects on leaf gas exchange properties
578 and daily C gain as discussed below. The above phenotype was rescued by complementing with
579 *CGR2* as seen in *cgr2com* or by overexpressing *CGR2* as in *CGR2OX*. Thus, the degree of
580 *CGR2* and *CGR3* mediated pectin methyl esterification can directly affect LMA by altering both
581 leaf thickness and leaf mass density.

582

583 ***CGR2* and *CGR3* Affect Area-Based Respiration and Daily C Gain by Altering LMD and** 584 **LMA**

585 In general, leaves growing under high light develop thicker leaves with multiple cell layers and
586 higher LMA (lower SLA) and incurs higher area-based respiration rates corresponding to their
587 greater mass per unit leaf area (Mitchell et al., 1999; Lambers et al., 2008). In contrast, plants
588 grown under low light have lower LMA (higher SLA) which optimizes light capture and lowers
589 area-based respiration rates (Lambers et al., 2008). This assists in maximizing daily C gain and
590 compensates for lower area-based photosynthesis rates when growing under low light conditions
591 (Lambers et al., 2008). Although *cgr2/3* produced thinner leaves, the marked enhancement in
592 area-based respiration positively correlated with enhanced leaf cell density and higher LMA.
593 Higher area-based respiratory rates led to smaller photosynthesis to respiration ratios, and when
594 coupled with smaller projected leaf area, they had a significant negative impact on daily carbon
595 gain. Thus, pectin methylesterification affects area-based respiration rates through alterations in
596 leaf cell density, LMD, and LMA and consequently affect photosynthetic efficiency in plants.

597

598 ***CGR2* and *CGR3* Directly Affect Area-Based Photosynthesis by Altering Mesophyll** 599 **Architecture**

600 Diffusion of CO₂ into chloroplasts occurs along the path which poses the least resistance through
601 the cell wall, plasma membrane, chloroplast envelope and into the chloroplast stroma (Terashima
602 et al., 2006). Therefore, S_c represents the active area through which CO₂ diffuses in to the
603 chloroplast stroma (Terashima et al., 2006). A decrease in S_c leads to a reduction in CO₂
604 concentration at rubisco and therefore to a reduction in the carboxylation to oxygenation ratio
605 (Terashima et al., 2006). Parameters that affect CO₂ diffusion into the chloroplast stroma are
606 thickness of the mesophyll cell wall, internal conductance to CO₂ diffusion, and stomatal

607 conductance (Terashima et al., 2006). S_c has been shown to be positively correlated with internal
608 conductance, while the latter is negatively correlated with cell wall thickness (Terashima et al.,
609 2006).

610
611 In contrast to our original hypothesis, area-based photosynthesis rates were significantly lower in
612 *cgr2/3* for most of the life cycle, even though this mutant possessed smaller projected leaf area
613 and denser leaves. The present study revealed that this reduction in area based photosynthesis in
614 *cgr2/3* was not a result of differences in chloroplast number and size, but, mainly a result of a
615 reduction in CO_2 partial pressure at rubisco due to restrictions imposed on CO_2 diffusion by
616 increased cell density and reduced airspaces in the leaf mesophyll which lowered S_c . Preliminary
617 investigations revealed that stomatal conductance is not negatively impacted in the mutant lines
618 examined during the present study (data not shown). Therefore, the observed reduction in area-
619 based photosynthetic rates is most probably due to a cumulative effect of lower S_c , higher
620 internal resistance and greater cell wall thickness per unit area. The greater area-based
621 photosynthesis rates in *cgr2/3* observed during early stages of vegetative development may have
622 been a result of leaves and cell walls being comparatively thinner in young plants. S_c values and
623 CO_2 partial pressure at rubisco in *cgr2/3* was restored to the levels of Col-0 in *cgr2com* owing to
624 alterations brought about by *CGR2* expression in its leaf anatomy: thicker leaves with less dense
625 mesophyll, more intercellular air spaces. S_c and CO_2 partial pressure in *CGR2OX* was similar to
626 that of Col-0. The lower area-based photosynthesis in *CGR2OX* may have resulted from thinner
627 but larger leaves which may have resulted in less photosynthetic machinery per unit leaf area.
628 Correspondingly, chloroplast number and size was lower in *CGR2OX*. These data emphasize the
629 importance of pectin methylesterification in fine tuning cell expansion and size and cell-to-cell
630 adhesion qualities in building a leaf mesophyll optimized for CO_2 exchange. While thin leaves
631 are associated with lower LMA (or enhanced SLA), it is important to maintain an optimum
632 thickness in order to maintain sufficient intercellular air spaces, which would maintain high
633 internal conductance, S_{mes} and S_c and therefore higher carboxylation rates.

634
635
636

637 **Pectin Methylesterification Mediates the Relationship Between Photosynthesis and Plant**
638 **Growth Through Alterations in C Partitioning to Leaf Area Growth and Thickening**

639 As hypothesized, suppression of *CGR2* and *CGR3* mediated pectin methylesterification had a
640 profound negative effect on leaf area growth while overexpression of *CGR2* significantly
641 enhanced leaf area growth. Suppression of *CGR2* and *CGR3* also led to a reduction in plant dry
642 weight. Overexpression of *CGR2* enhanced plant dry weight. Growth modelling revealed that the
643 observed variations in growth were not caused by changes in area-based photosynthesis. In fact,
644 high rates of area-based photosynthesis measured in *cgr2/3* during early growth were found to be
645 sufficient to drive growth higher than that seen in Col-0. Thus, growth had the opposite trend
646 ($CGROX > Col-0 > cgr2/3$) compared with area-based photosynthetic rate ($cgr2/3 > Col-$
647 $0 > CGROX$). In order to account for enhanced overall plant growth, the amount of net
648 assimilated C available for growth has to increase which will depend on the total amount of C
649 assimilated and the amount of C respired to support maintenance processes (Weraduwege et al.,
650 2015). Our study showed that *CGR2* and *CGR3*, through pectin methylesterification, is capable
651 of affecting total C assimilation by directly altering leaf area growth and by altering maintenance
652 respiratory costs through direct effects on LMA. We also showed that although *CGR2* and *CGR3*
653 affect area-based photosynthetic rates, it is not a major factor affecting overall plant growth.

654
655 A reduction in pectin methylesterification by reduced expression of *CGR2* and *CGR3* seem to
656 enhance cell wall hardening and cell-to-cell adhesion through increased cross-linking between
657 galacturonic acid and Ca^{2+} , favoring an increase in LMA against cell expansion and posing a
658 greater demand for C for LMA growth compared to area growth (**Fig. 12A**). Hence less C will be
659 utilized in area growth of new leaves and more C will be utilized in increasing LMA leading to a
660 smaller projected leaf area (**Fig. 12A**). Smaller projected leaf area yields lower whole plant C
661 assimilation. In contrast, an increase in pectin methylesterification via enhanced expression of
662 *CGR2* and *CGR3* seem to reduce cell wall hardening and cell-to-cell adhesion and thereby
663 favoring cell expansion and area growth against increases in LMA and posing a greater demand
664 for C for leaf area growth compared to that for LMA growth (**Fig. 12B**). Hence more C will be
665 utilized in area growth of new leaves and a lower proportion C will be utilized in LMA growth
666 leading to larger projected leaf area and enhanced whole plant C assimilation (**Fig. 12B**).
667 Suppression of *CGR2* and *CGR3* increases respiratory costs through higher LMA resulting in

668 lower photosynthesis: respiration ratios, lower daily C gain, reduced net assimilated C available
669 for growth and ultimately reduced plant growth (**Fig. 12A**); overexpression of *CGR2* yields
670 opposite physiological effects (**Fig. 12B**).

671
672 There may be other genes that may also impact partition of carbon toward leaf area growth or
673 LMA. One example is the xyloglucan endotransglucosylase/ hydrolase (*XTH*) gene family.
674 Reduced expression of *XTH8* and *XTH31* gene expression led to reduced leaf width, length, and
675 leaf area (Miura and Hasegawa, 2010). The leaf mesophyll of these mutant lines consisted of a
676 large number of small mesophyll cells per unit area (Miura and Hasegawa, 2010). Suppression of
677 *XTH21* led to a reduction in cellulose, and xyloglucan content with subsequent reductions in
678 both leaf and plant size (Liu et al., 2007). One of the major roles of XTH enzymes is cleavage of
679 cross-linkages between cellulose and hemicellulose microfibrils which promotes wall loosening
680 and cell expansion. This may explain the above leaf phenotypes in *xth8*, *xth21*, and *xth31* mutant
681 lines (Liu et al., 2007; Miura and Hasegawa, 2010). Thus, through its effects on cell wall
682 properties, *XTH* genes may be able to alter C partitioning to leaf area and thickening and thereby
683 affect overall plant growth similar to the role played by *CGR* genes.

684
685 In summary, results from the present study are in agreement with findings from Weraduwege et
686 al. (2015) that optimization of leaf area growth and plant growth can be achieved by increased
687 partitioning of C to leaf area growth with concomitant reduction in partitioning to growth in
688 terms of LMA especially during the early vegetative growth phase (Weraduwege et al., 2015)
689 and that photosynthesis drives growth through alterations in C partitioning to leaf area and LMA
690 growth. In the present study we found that *CGR2* and *CGR3* directly affect this relationship by
691 altering the degree of cell expansion and/or adhesion thereby driving C partitioning by
692 generating C demands for leaf area growth and for growth in terms of LMA.

693 694 **CONCLUSION**

695 Our study supports the model that qualitative and quantitative changes in pectin in the cell wall
696 have a significant impact on area-based photosynthesis and respiration through alterations in leaf
697 thickness, mesophyll cell density, and area of the leaf blade. Such changes in mesophyll
698 architecture directly altered LMA and consequently area-based respiration. *CGR2* and *CGR3*

699 affected area-based photosynthesis by altering CO₂ availability at rubisco. These genes could
700 affect plant-based photosynthesis by enabling enhanced light capture through larger leaf area.
701 These data emphasizes the importance of pectin methylesterification in fine-tuning cell
702 expansion and size, and adhesion qualities when building an optimum leaf to maximize
703 photosynthesis under different environmental conditions. While thin leaves are associated with
704 reduced LMA, it is important to maintain an optimum thickness in order to maintain sufficient
705 intercellular air spaces that would maintain high internal conductance as reflected in S_{mes} and S_c
706 and therefore higher carboxylation rates. *CGR2* and *CGR3*, which directly alter the size of the
707 leaf blade and mesophyll architecture, may find applications in the future to improve light
708 interception in crop plant canopies.

709
710 Overexpression of *CGR2* has had a significant positive effect on leaf area and plant growth.
711 Suppression of *CGR2* and *CGR3* caused a marked increase in LMA, and a reduction in leaf area
712 and plant growth. These differences resulted through changes in C partitioning to leaf area
713 growth and growth in terms of LMA and not as a result of altered area-based photosynthesis
714 rates. Therefore, photosynthesis drives plant growth through alterations in C partitioning to new
715 leaf area growth and LMA growth, and the present study discovered that pectin
716 methylesterification affects this relationship by directly altering the degree of cell expansion and
717 positioning in the leaves to create dynamic carbon demands in leaf area growth and leaf mass
718 thereby driving carbon partitioning for these processes. Collectively, these results uncover an
719 unexpected connection between cell wall composition and photosynthesis and support the novel
720 model that through its role in modulation of organ development, the cell wall plasticity is a key
721 factor influencing photosynthetic processes in land plants.

722

723 **SUPPLEMENTAL DATA**

724 **Supplemental Figure S1.** Cell wall composition in *Arabidopsis* with altered *CGR2* and *CGR3*
725 expression.

726 **Supplemental Figure S2.** Hypocotyl and rosette size in *Arabidopsis* with altered *CGR2* and
727 *CGR3* expression.

728 **Supplemental Figure S3.** Early growth phenotypes in *Arabidopsis* with altered *CGR2* and
729 *CGR3* expression.

730 **Supplemental Figure S4.** Partitioning of photosynthetic C to shoots and roots in *Arabidopsis*
731 with altered *CGR2* and *CGR3* expression.

732

733 **ACKNOWLEDGEMENTS**

734 We are grateful to Drs. Sean E. Weise, (Department of Biochemistry and Molecular Biology),
735 Cliff Foster (the Cell Wall Facility, Great Lakes Bioenergy Research Center), Alicia Withrow
736 and Melinda Frame (Center for Advanced Microscopy) of Michigan State University (East
737 Lansing, MI), and to Dr. Suvankar Chakraborty (Stable Isotope Ratio Facility for Environmental
738 Research) of University of Utah for their support. We also wish to thank Jim Klug and Cody
739 Keilen (Growth Chamber Facility) of Michigan State University for their assistance and all
740 members of the Sharkey and Brandizzi labs for their support.

741

742 **FIGURE LEGENDS**

743 **Figure 1. Projected and total leaf area over time in *Arabidopsis* with altered *CGR2* and**
744 ***CGR3* expression. (A) Projected leaf area and (B) total leaf area at 4 different harvests (H) is**
745 **presented for Col-0, *cgr2com*, *CGR2OX*, and *cgr2/3*. H1, H2, H3, and H4 correspond to 29, 49,**
746 **63, and 82 DAS, respectively. For clarity, data for H1 is presented as inserts in A and B. Values**
747 **represent the mean \pm SE and n = 5 plants per line. Statistical differences at $\alpha = 0.05$ are marked**
748 **with lower case letters.**

749

750 **Figure 2. Leaf thickness and anatomy in *Arabidopsis* with altered *CGR2* and *CGR3***
751 **expression. (A) Representative micrographs of leaf cross sections, (B) leaf thickness, (C) the**
752 **relationship between the number of mesophyll cells and size of the intercellular air spaces in the**
753 **leaf mesophyll, (D) the surface area of mesophyll cells exposed to intercellular air spaces per**
754 **unit leaf area (S_{mes}), and (E) the surface area of chloroplasts exposed to intercellular air spaces**
755 **per unit leaf area (S_c) are presented for Col-0, *cgr2com*, *CGR2OX*, and *cgr2/3*. In (A), leaf**
756 **thickness is denoted by red double arrows. Data were obtained from 34-day old leaves. In (B),**
757 **(D), and (E) values represent the mean \pm SE and n = 4 plants per line. In (C) n = 4 plants per line**
758 **were used to obtain the mean values for the area of air spaces as a % of area of leaf cross section**
759 **and the number of mesophyll cells per mm^2 of leaf cross section. Statistical differences at $\alpha =$**
760 **0.05 are marked with lower case letters.**

761 **Figure 3. Abundance and size of chloroplasts in *Arabidopsis* with altered *CGR2* and *CGR3***
762 **expression. (A)** The number of chloroplasts per unit area of leaf cross section and **(B)** size of
763 chloroplasts in 34-day old leaves is shown for Col-0, *cgr2com*, *CGR2OX*, and *cgr2/3*. Values
764 represent the mean \pm SE and n = 12. Statistical differences at $\alpha = 0.05$ are marked with lower
765 case letters.

766
767 **Figure 4. Photosynthesis and respiration overtime in *Arabidopsis* with altered *CGR2* and**
768 ***CGR3* expression. (A)** Area-based photosynthesis, **(B)** area-based nighttime respiration, **(C)**
769 photosynthesis on a whole plant basis, and **(D)** nighttime respiration on a whole plant basis at 4
770 different harvests (H) is shown for Col-0, *cgr2com*, *CGR2OX*, and *cgr2/3*. Photosynthesis (C
771 gain) is shown as a positive number **(A and C)** while respiration (C loss) is shown as a negative
772 number **(B and D)**. H1, H2, H3 and H4 correspond to 29, 49, 63 and 82 DAS, respectively.
773 Values represent the mean \pm SE and n = 5 plants per line. Statistical differences at $\alpha = 0.05$ are
774 marked with lower case letters.

775
776 **Figure 5. The daily C gain in *Arabidopsis* with altered *CGR2* and *CGR3* expression. (A)**
777 Photosynthesis to respiration ratio at 4 different harvests (H) and **(B)** the daily C gain at 2
778 different harvests for Col-0, *cgr2com*, *CGR2OX*, and *cgr2/3* is given. H1, H2, H3 and H4
779 correspond to 29, 49, 63 and 82 DAS, respectively. Values represent the mean \pm SE and n = 5
780 plants per line. Statistical differences at $\alpha = 0.05$ are marked with lower case letters.

781
782 **Figure 6. The degree of resistance to CO₂ diffusion through the leaf mesophyll overtime in**
783 ***Arabidopsis* with altered *CGR2* and *CGR3* expression. (A-C)** The $\delta^{13}\text{C}_{\text{VPDB}}$ value calculated as
784 the ratio of ¹³C to ¹²C isotopes in leaf tissue relative to a Vienna-Pee-Dee Belemnite standard
785 (VPDB), and **(D-F)** CO₂ partial pressure at rubisco at 3 different harvests (H) is shown for Col-0,
786 *cgr2com*, *CGR2OX*, and *cgr2/3*. H2, H3, and H4 correspond to 49, 63 and 82 DAS, respectively.
787 Values represent the mean \pm SE and n = 5 plants per line. Statistical differences at $\alpha = 0.05$ are
788 marked with lower case letters.

789

790 **Figure 7. Variations in leaf growth parameters overtime in *Arabidopsis* with altered *CGR2***
791 **and *CGR3* expression. (A)** Leaf mass per unit leaf area or LMA, **(B)** leaf area ratio, **(C)** leaf
792 mass ratio, and **(D)** root mass ratio at 4 different harvests (H) for Col-0, *cgr2com*, *CGR2OX*, and
793 *cgr2/3* is presented. H1, H2, H3 and H4 correspond to 29, 49, 63 and 82 DAS, respectively.
794 Values represent the mean and n = 5 plants per line. Statistical differences at $\alpha = 0.05$ are marked
795 with lower case letters.

796
797 **Figure 8. Variations in dry weight overtime in *Arabidopsis* with altered *CGR2* and *CGR3***
798 **expression. (A)** Leaf, **(B)** root, **(C)** inflorescence, and **(D)** whole plant dry weight at 4 different
799 harvests (H) for Col-0, *cgr2com*, *CGR2OX*, and *cgr2/3* is given. H1, H2, H3 and H4 correspond
800 to 29, 49, 63 and 82 DAS, respectively. Values represent the mean \pm SE and n = 5 plants per line.
801 Statistical differences at $\alpha = 0.05$ are marked with lower case letters.

802
803 **Figure 9. Modeled relative growth rates overtime in *Arabidopsis* with altered *CGR2* and**
804 ***CGR3* expression. (A)** Area-based relative growth rates and **(B)** mass-based relative growth
805 rates simulated from day 5-84 using the *Arabidopsis* Leaf Area Growth Model fitted with data
806 obtained from Col-0, *cgr2com*, *CGR2OX*, and *cgr2/3* is presented.

807
808 **Figure 10. Modeled C partitioning to growth and respiration in *Arabidopsis* with altered**
809 ***CGR2* and *CGR3* expression. C** partitioned to support growth in terms of leaf area and LMA,
810 and inflorescence growth, root growth, and maintenance and growth respiration is presented as
811 percentages of the daily available C at 29, 49, 63 and 82 DAS. Data was derived from the
812 *Arabidopsis* Leaf Area Growth Model fitted with data obtained from Col-0, *cgr2com*, *CGR2OX*,
813 and *cgr2/3*.

814
815 **Figure 11. Comparison of the effects of altered area-based photosynthesis and C**
816 **partitioning coefficients on plant growth in *Arabidopsis* with altered *CGR2* and *CGR3***
817 **expression. Modeled effects on leaf area and leaf, root, and plant dry weights when either**
818 photosynthetic rates or partitioning coefficients spanning the entire growth cycle for Col-0 is
819 replaced by that of **(A)** *CGR2OX* and **(B)** *cgr2/3* are presented. In **(A)** and **(B)**, blue lines
820 represent modeled growth for Col-0 and red squares represent measured data points (mean \pm SD)

821 for Col-0 at 29, 49, 63, and 82 DAS. Grey lines represent modeled data for Col-0 when its area-
822 based photosynthesis rates are replaced by that of either CGR2OX (A) or cgr2/3 (B). Orange
823 lines represent modeled data for Col-0 when its partitioning coefficients (Table 1) are replaced
824 by that of either CGR2OX (A) or cgr2/3 (B) without making any changes to area-based
825 photosynthesis rates of Col-0. In (A), asterisks represent measured data for CGR2OX at 63 and
826 82 DAS. In (B), the dotted line indicates the upper limit of measured data for cgr2/3.

827

828 **Figure 12. CGR2 and CGR3 mediated pectin methylesterification regulates the relationship**
829 **between photosynthesis and plant growth.** A schematic diagram outlining how (A)

830 suppression or (B) overexpression of *CGR2* and *CGR3* gene expression affects the relationship
831 between photosynthesis and plant growth in *Arabidopsis thaliana* is presented. Suppression of
832 *CGR2* and *CGR3* reduces the degree of pectin methylation which leads to an increase in cell-to-
833 cell adhesion, cation mediated cross linking of galacturonic acid and consequent hardening of
834 cell walls. *CGR2* overexpression increases the degree of pectin methylation which allows cell
835 expansion through reduced cell-to-cell adhesion and cation mediated cross-linking. We propose
836 that pectin methyltransferase enzyme, through its ability to directly alter cell expansion,
837 determines the amount of C partitioned to leaf area growth vs. growth in terms of leaf mass per
838 unit area (LMA). For example, while more C is partitioned to growth in terms of LMA in the
839 *CGR2* and *CGR3* double knockout mutant, in the *CGR2* overexpression line more C is
840 partitioned to leaf area growth. An increase in LMA leads to enhanced area-based respiration and
841 a reduction in leaf area contribute to a reduction in whole plant photosynthesis. Collectively, this
842 results in a reduction in C available for growth and consequently a decrease in overall plant
843 growth; an opposite trend is seen in *CGR2OX*. Thus, *CGR2* and *CGR3* through their ability to
844 alter the degree of methylated pectin in the cell wall of the mesophyll cells, determines how
845 photosynthate is utilized to grow the plant. In other words, *CGR2* and *CGR3* mediated pectin
846 methylesterification affects the relationship between photosynthesis and plant growth by
847 regulating the proportions of C that is partitioned to leaf area growth and LMA. Final overall
848 growth mainly depends on the expression patterns of *CGR2* and *CGR3* and how much C is
849 partitioned to area growth and LMA and not on area-based photosynthesis. Abbreviations: PME
850 – pectin methylesterase, PMEI – PME inhibitor, PMT – pectin methyltransferase. CH₃OH is
851 methanol.

852 REFERENCES

- 853 **Amthor JS** (1984) The role of maintenance respiration in plant growth. *Plant Cell Environ* **7**:
854 561-569
- 855 **Burton RA, Gibeaut DM, Bacic A, Findlay K, Roberts K, Hamilton A, Baulcombe DC,**
856 **Fincher GB** (2000) Virus-induced silencing of a plant cellulose synthase gene. *Plant Cell*
857 **12**: 691-705
- 858 **Caffall KH, Mohnen D** (2009) The structure, function, and biosynthesis of plant cell wall pectic
859 polysaccharides. *Carbohydr Res* **344**: 1879-1900
- 860 **Cunningham SA, Summerhayes B, Westoby M** (1999) Evolutionary divergences in leaf
861 structure and chemistry, comparing rainfall and soil nutrient gradients. *Ecol Monogr* **69**:
862 569-588
- 863 **De Vries FWTP, Brunsting AHM, Van Laar HH** (1974) Products, requirements and
864 efficiency of biosynthesis a quantitative approach. *J Theor Biol* **45**: 339-377
- 865 **Evans JR, Caemmerer Sv, Setchell BA, Hudson GS** (1994) The relationship between CO₂
866 transfer conductance and leaf anatomy in transgenic tobacco with a reduced content of
867 rubisco. *Aust J Plant Physiol* **21**: 475-495
- 868 **Farquhar G, Ehleringer J, Hubick K** (1989) Carbon isotope discrimination and
869 photosynthesis. *Annu Rev Plant Physiol Plant Mol Biol* **40**: 503-537
- 870 **Farquhar G, O'Leary M, Berry J** (1982) On the relationship between carbon isotope
871 discrimination and the intercellular carbon dioxide concentration in leaves. *Funct Plant*
872 *Biol* **9**: 121-137
- 873 **Galmés J, Ochogavía JM, Gago J, Roldán EJ, Cifre J, Conesa MÀ** (2013) Leaf responses to
874 drought stress in mediterranean accessions of *Solanum lycopersicum*: anatomical
875 adaptations in relation to gas exchange parameters. *Plant Cell Environ* **36**: 920-935
- 876 **Heldt H-W, Piechulla B** (2010) *Plant Biochemistry*, Ed 4. Academic Press, London, UK
- 877 **Honda H, Fisher JB** (1978) Tree branch angle: maximizing effective leaf area. *Science* **199**:
878 888-890
- 879 **Kim HS, Delaney TP** (2002) Over-expression of TGA5, which encodes a bZIP transcription
880 factor that interacts with NIM1/NPR1, confers SAR-independent resistance in
881 *Arabidopsis thaliana* to *Peronospora parasitica*. *Plant J* **32**: 151-163

- 882 **Kim S-J, Held MA, Zemelis S, Wilkerson C, Brandizzi F** (2015) CGR2 and CGR3 have
883 critical overlapping roles in pectin methylesterification and plant growth in *Arabidopsis*
884 *thaliana*. *Plant J* **82**: 208-220
- 885 **Lambers H, Chapin F, Pons T** (2008) *Plant Physiological Ecology*, Ed 2. Springer., NewYork,
886 NY
- 887 **Lionetti V, Raiola A, Camardella L, Giovane A, Obel N, Pauly M, Favaron F, Cervone F,**
888 **Bellincampi D** (2007) Overexpression of pectin methylesterase inhibitors in *Arabidopsis*
889 restricts fungal infection by *Botrytis cinerea*. *Plant Physiol* **143**: 1871-1880
- 890 **Liu YB, Lu SM, Zhang JF, Liu S, Lu YT** (2007) A xyloglucan endotransglucosylase/hydrolase
891 involves in growth of primary root and alters the deposition of cellulose in *Arabidopsis*.
892 *Planta* **226**: 1547-1560
- 893 **Mariko S** (1988) Maintenance and constructive respiration in various organs of *Helianthus*
894 *annuus* L. and *Zinnia elegans* L. *Bot Mag* **101**: 73
- 895 **Mitchell KA, Bolstad PV, Vose JM** (1999) Interspecific and environmentally induced variation
896 in foliar dark respiration among eighteen southeastern deciduous tree species. *Tree*
897 *Physiol* **19**: 861-870
- 898 **Miura K, Hasegawa PM** (2010) Sumoylation and other ubiquitin-like post-translational
899 modifications in plants. *Trends Cell Biol* **20**: 223-232
- 900 **Pilling J, Willmitzer L, Bucking H, Fisahn J** (2004) Inhibition of a ubiquitously expressed
901 pectin methyl esterase in *Solanum tuberosum* L. affects plant growth, leaf growth
902 polarity, and ion partitioning. *Planta* **219**: 32-40
- 903 **Poorter H, Niinemets U, Poorter L, Wright IJ, Villar R** (2009) Causes and consequences of
904 variation in leaf mass per area (LMA): a meta-analysis. *New Phytol* **182**: 565-588
- 905 **Shiple B** (2002) Trade-offs between net assimilation rate and specific leaf area in determining
906 relative growth rate: relationship with daily irradiance. *Funct Ecol* **16**: 682-689
- 907 **Terashima I, Hanba YT, Tazoe Y, Vyas P, Yano S** (2006) Irradiance and phenotype:
908 comparative eco-development of sun and shade leaves in relation to photosynthetic CO₂
909 diffusion. *J Exp Bot* **57**: 343-354
- 910 **Thomas RB, Reid CD, Ybema R, Strain BR** (1993) Growth and maintenance components of
911 leaf respiration of cotton grown in elevated carbon dioxide partial pressure. *Plant Cell*
912 *Environ* **16**: 539-546

- 913 **Tsuge T, Tsukaya H, Uchimiya H** (1996) Two independent and polarized processes of cell
914 elongation regulate leaf blade expansion in *Arabidopsis thaliana* (L.) Heynh.
915 *Development* **122**: 1589-1600
- 916 **Villar R, Ruiz-Robledo J, Ubera JL, Poorter H** (2013) Exploring variation in leaf mass per
917 area (LMA) from leaf to cell: an anatomical analysis of 26 woody species. *Am J Bot* **100**:
918 1969-1980
- 919 **Weraduwege SM, Chen J, Anozie FC, Morales A, Weise SE, Sharkey TD** (2015) The
920 relationship between leaf area growth and biomass accumulation in *Arabidopsis thaliana*.
921 *Front Plant Sci* **6**
- 922 **Witkowski ETF, Lamont B** (1991) Leaf specific mass confounds leaf density and thickness.
923 *Oecologia* **88**: 486-493
- 924 **Wolf S, Mouille G, Pelloux J** (2009) Homogalacturonan methyl-esterification and plant
925 development. *Molecular Plant* **2**: 851-860
- 926 **Xiao C, Anderson CT** (2013) Roles of pectin in biomass yield and processing for biofuels.
927 *Front Plant Sci* **4**
928
929

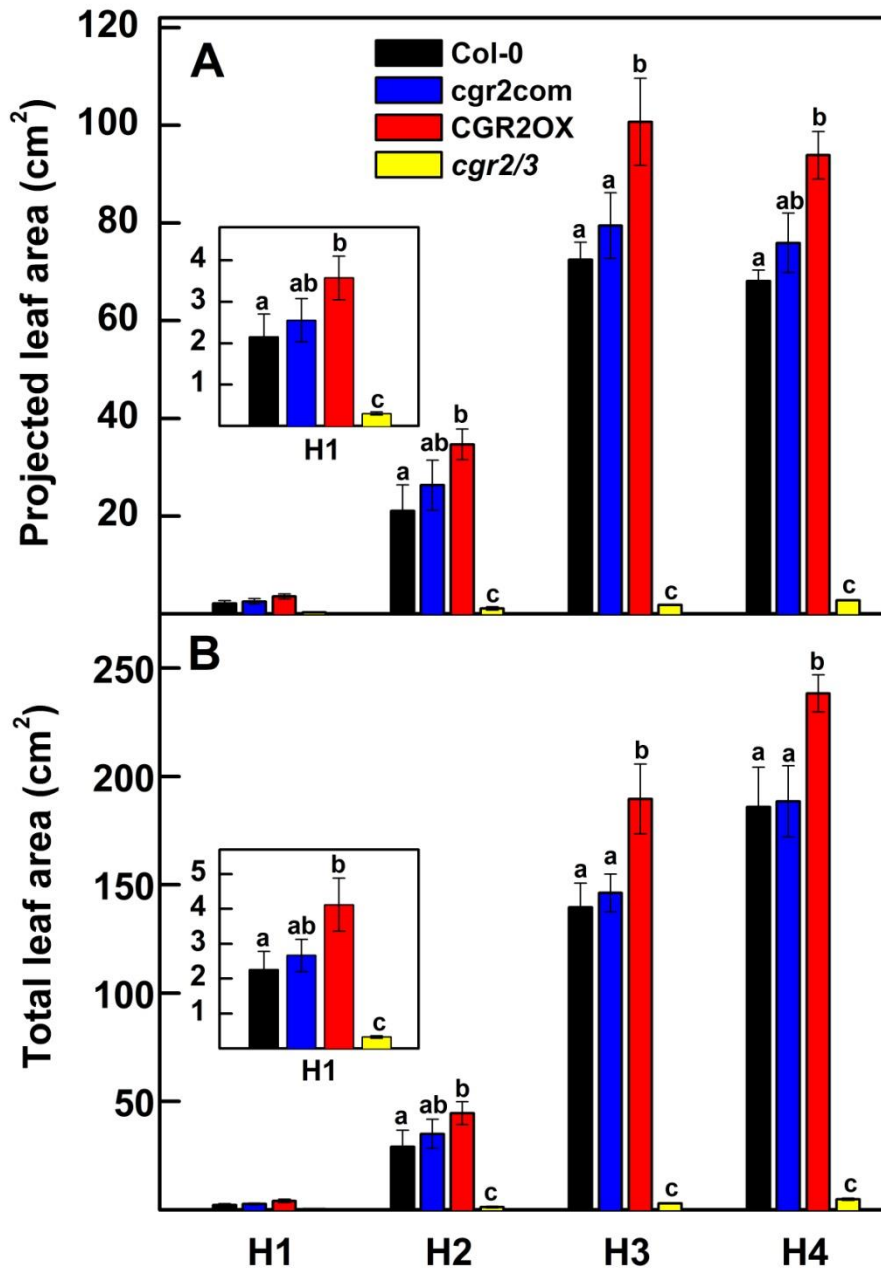
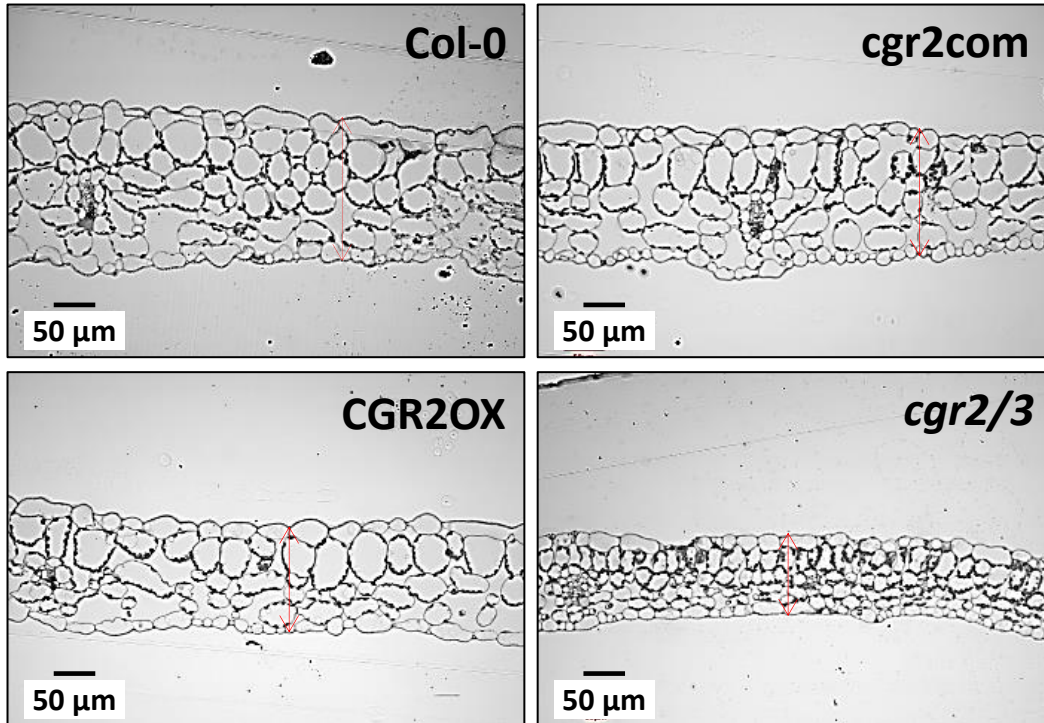


Figure 1. Projected and total leaf area over time in *Arabidopsis* with altered *CGR2* and *CGR3* expression. (A) Projected leaf area and (B) total leaf area at 4 different harvests (H) is presented for Col-0, *cgr2com*, *CGR2OX*, and *cgr2/3*. H1, H2, H3, and H4 correspond to 29, 49, 63, and 82 DAS, respectively. For clarity, data for H1 is presented as inserts in A and B. Values represent the mean \pm SE and $n = 5$ plants per line. Statistical differences at $\alpha = 0.05$ are marked with lower case letters.

A



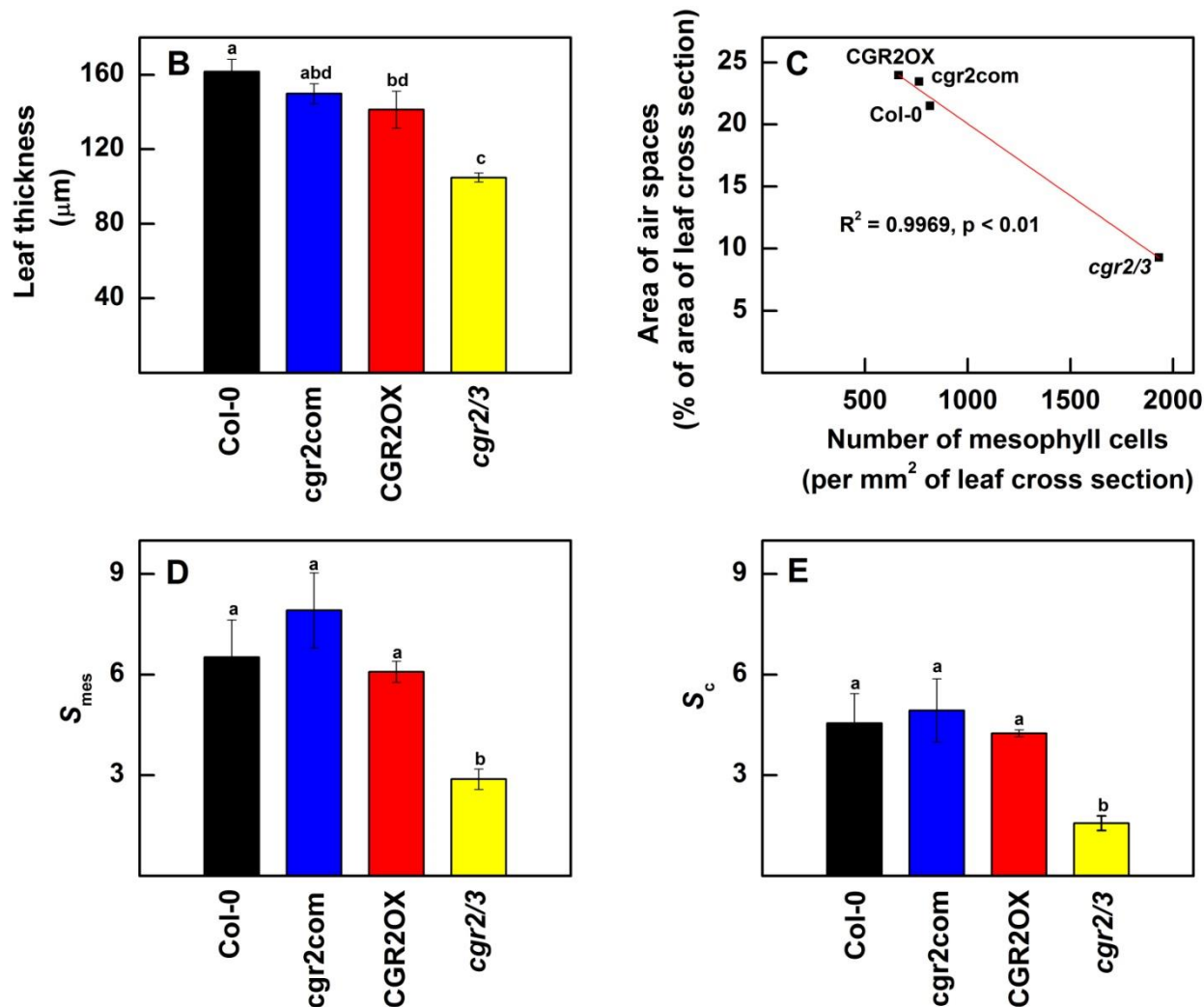


Figure 2. Leaf thickness and anatomy in *Arabidopsis* with altered *CGR2* and *CGR3* expression. (A) Representative micrographs of leaf cross sections, (B) leaf thickness, (C) the relationship between the number of mesophyll cells and size of the intercellular air spaces in the leaf mesophyll, (D) the surface area of mesophyll cells exposed to intercellular air spaces per unit leaf area (S_{mes}), and (E) the surface area of chloroplasts exposed to intercellular air spaces per unit leaf area (S_c) are presented for Col-0, cgr2com, CGR2OX, and cgr2/3. In (A), leaf thickness is denoted by red double arrows. Data were obtained from 34-day old leaves. In (B), (D), and (E) values represent the mean \pm SE and $n = 4$ plants per line. In (C) $n = 4$ plants per line were used to obtain the mean values for the area of air spaces as a % of area of leaf cross section and the number of mesophyll cells per mm² of leaf cross section. Statistical differences at $\alpha = 0.05$ are marked with lower case letters.

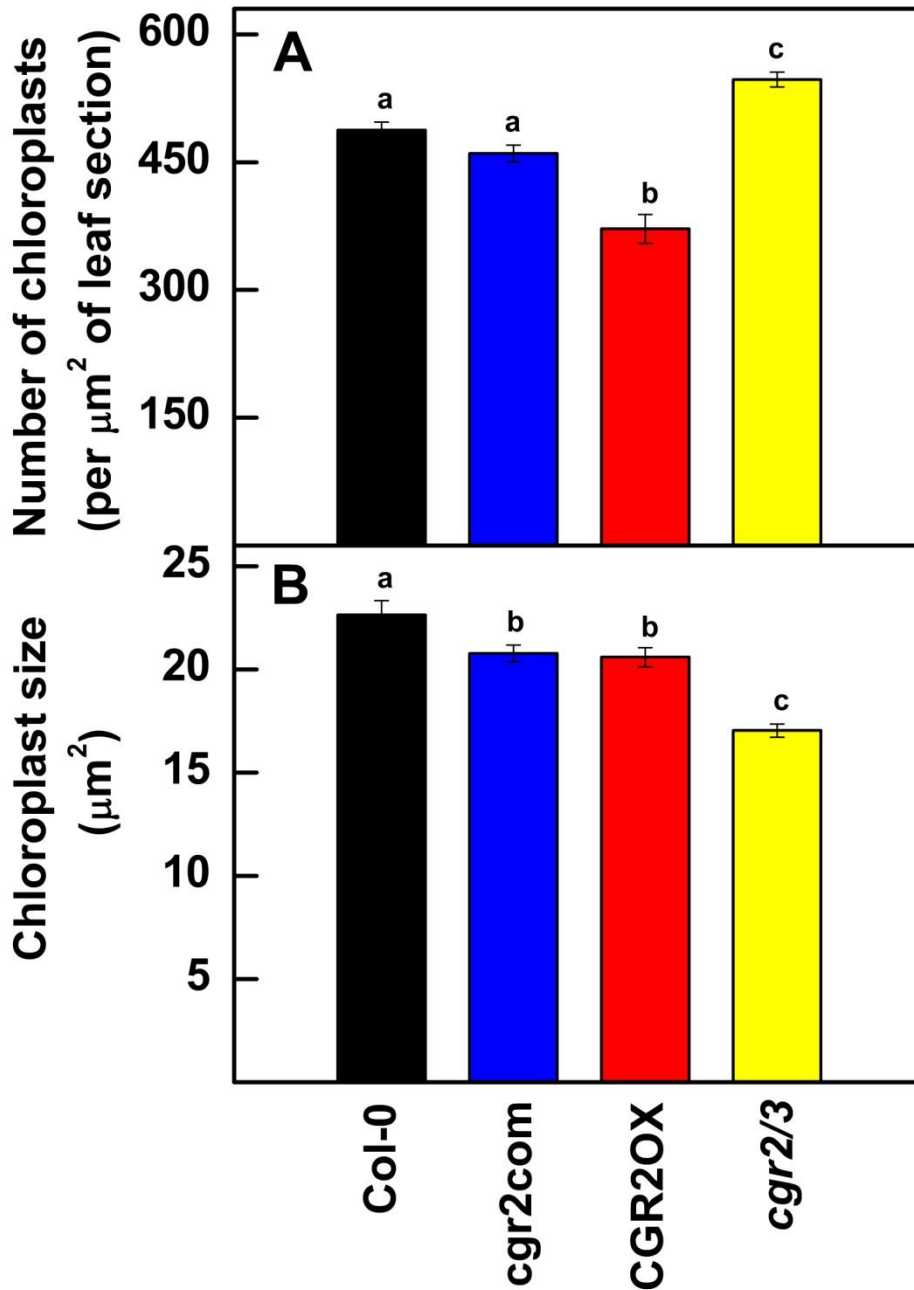


Figure 3. Abundance and size of chloroplasts in *Arabidopsis* with altered *CGR2* and *CGR3* expression. (A) The number of chloroplasts per unit area of leaf cross section and (B) size of chloroplasts in 34-day old leaves is shown for Col-0, cgr2com, CGR2OX, and cgr2/3. Values represent the mean \pm SE and $n = 12$. Statistical differences at $\alpha = 0.05$ are marked with lower case letters.

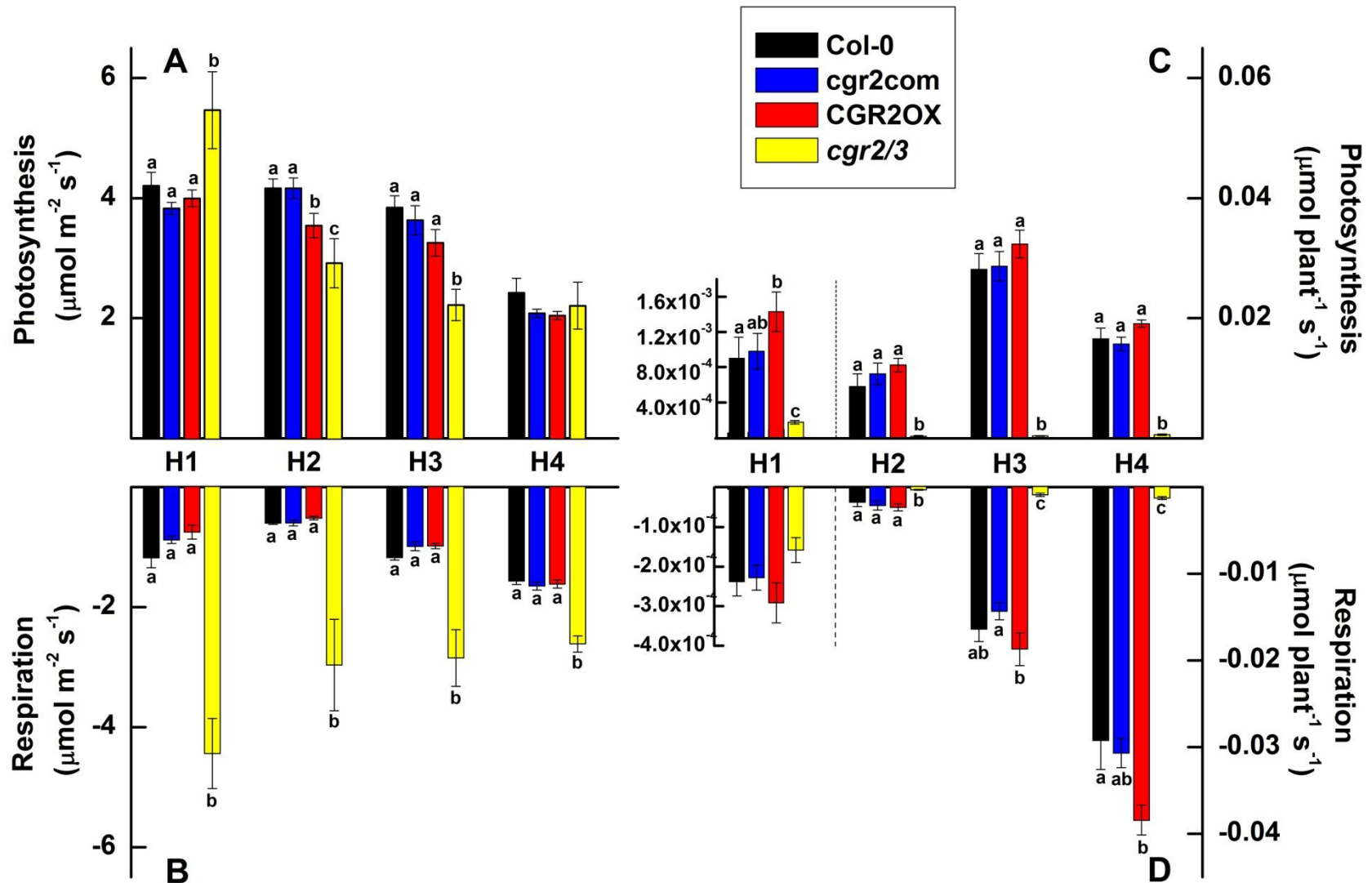


Figure 4. Photosynthesis and respiration overtime in *Arabidopsis* with altered *CGR2* and *CGR3* expression. (A) Area-based photosynthesis, (B) area-based nighttime respiration, (C) photosynthesis on a whole plant basis and (D) nighttime respiration on a whole plant basis at 4 different harvests (H) is shown for Col-0, *cgr2com*, *CGR2OX*, and *cgr2/3*. Photosynthesis (C gain) is shown as a positive number (A and C) while respiration (C loss) is shown as a negative number (B and D). H1, H2, H3 and H4 correspond to 27, 46, 65, and 92 DAS, respectively. Values represent the mean \pm SE and $n = 5$ plants per line. Statistical differences at $\alpha = 0.05$ are marked with lower case letters.

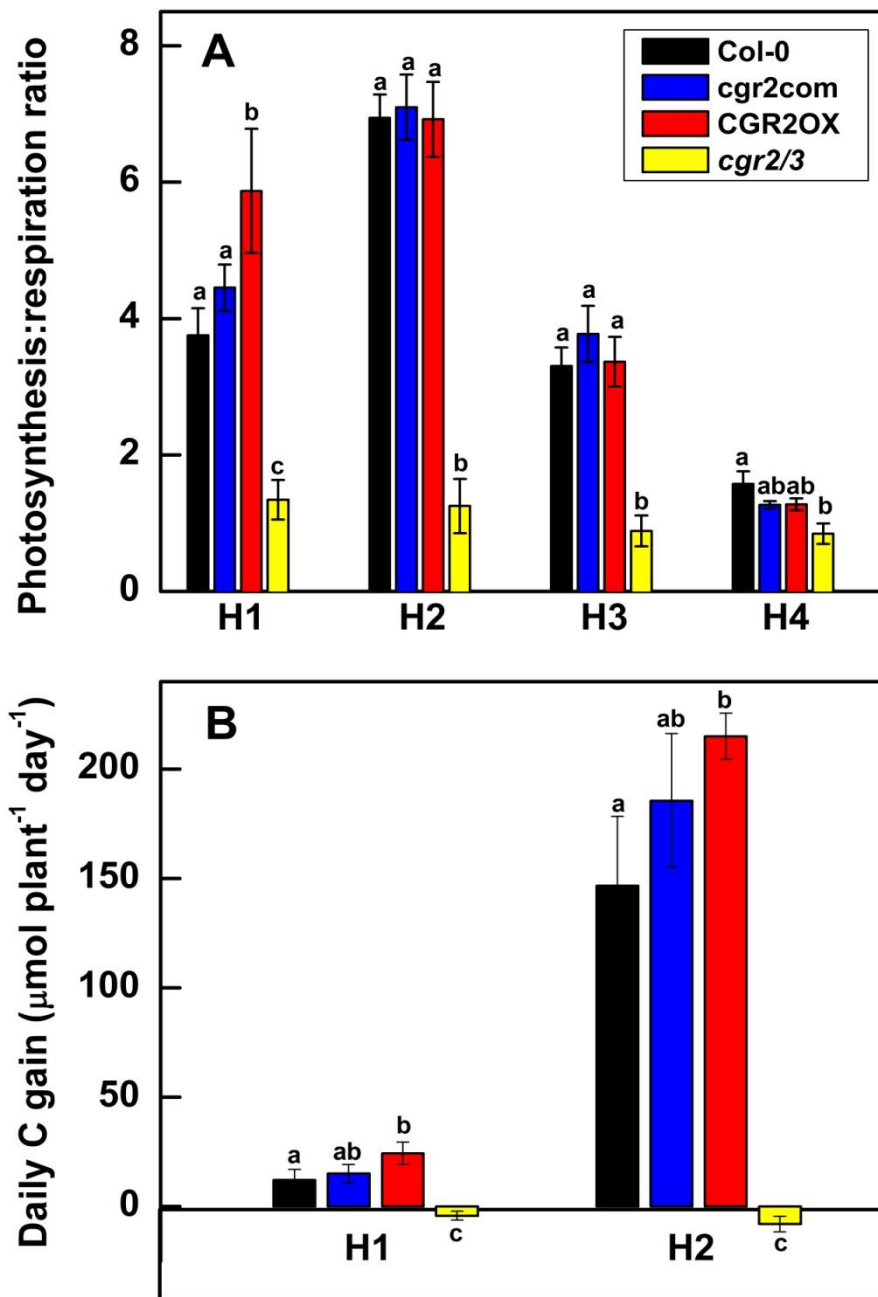


Figure 5. The daily C gain in *Arabidopsis* with altered *CGR2* and *CGR3* expression. (A) Photosynthesis to respiration ratio at 4 different harvests (H) and (B) the daily C gain at 2 different harvests for Col-0, *cgr2com*, *CGR2OX*, and *cgr2/3* is given. H1, H2, H3 and H4 correspond to 29, 49, 63 and 82 DAS, respectively. Values represent the mean \pm SE and $n = 5$ plants per line. Statistical differences at $\alpha = 0.05$ are marked with lower case letters.

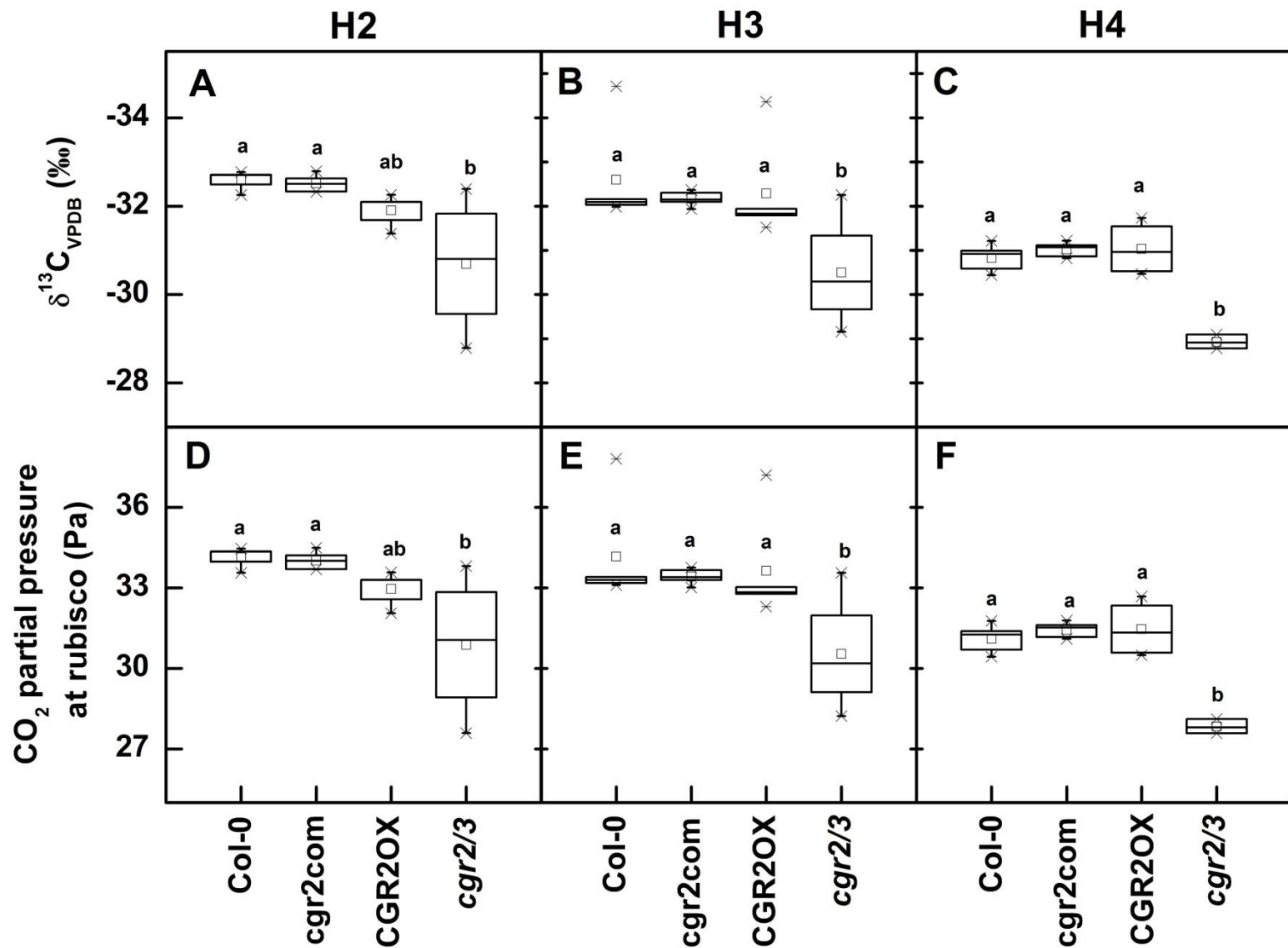


Figure 6. The degree of resistance to CO_2 diffusion through the leaf mesophyll overtime in *Arabidopsis* with altered *CGR2* and *CGR3* expression. (A-C) The $\delta^{13}\text{C}_{\text{VPDB}}$ value calculated as the ratio of ^{13}C to ^{12}C isotopes in leaf tissue relative to a Vienna-Pee-Dee Belemnite standard (VPDB), and (D-F) CO_2 partial pressure at rubisco at 3 different harvests (H) is shown for Col-0, cgr2com, CGR2OX, and cgr2/3 at H2, H3, and H4, respectively. Values represent the mean \pm SE and $n = 5$ plants per line. Statistical differences at $\alpha = 0.05$ are marked with lower case letters.

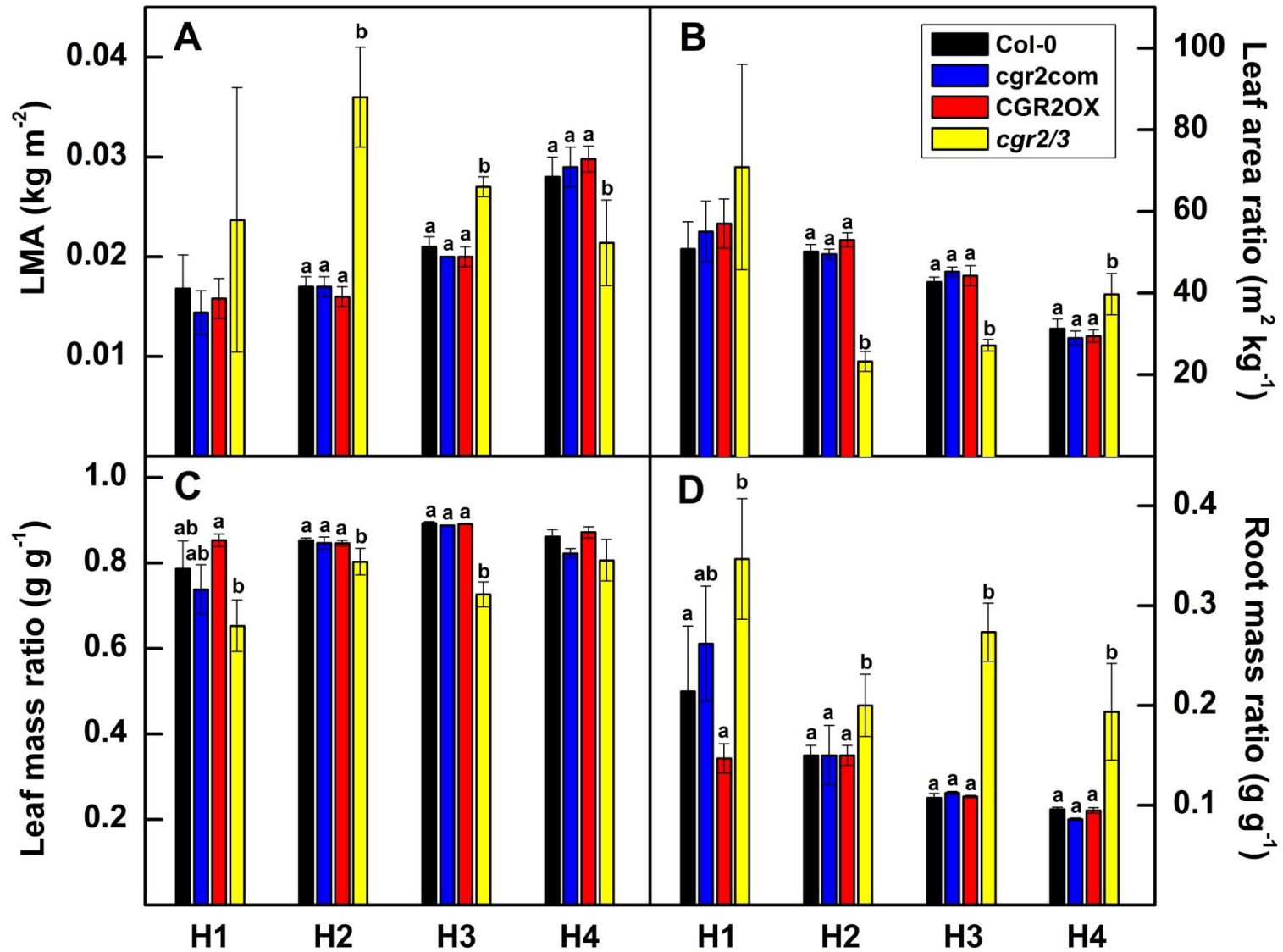


Figure 7. Variations in leaf growth parameters overtime in *Arabidopsis* with altered *CGR2* and *CGR3* expression. (A) Leaf mass per unit leaf area or LMA, (B) leaf area ratio, (C) leaf mass ratio, and (D) root mass ratio at 4 different harvests (H) for Col-0, *cgr2com*, *CGR2OX*, and *cgr2/3* is presented. H1, H2, H3 and H4 correspond to 29, 49, 63 and 82 DAS, respectively. Values represent the mean and error bars represent standard deviation. Letters above bars indicate significant differences ($P < 0.05$) are marked with lower case letters.

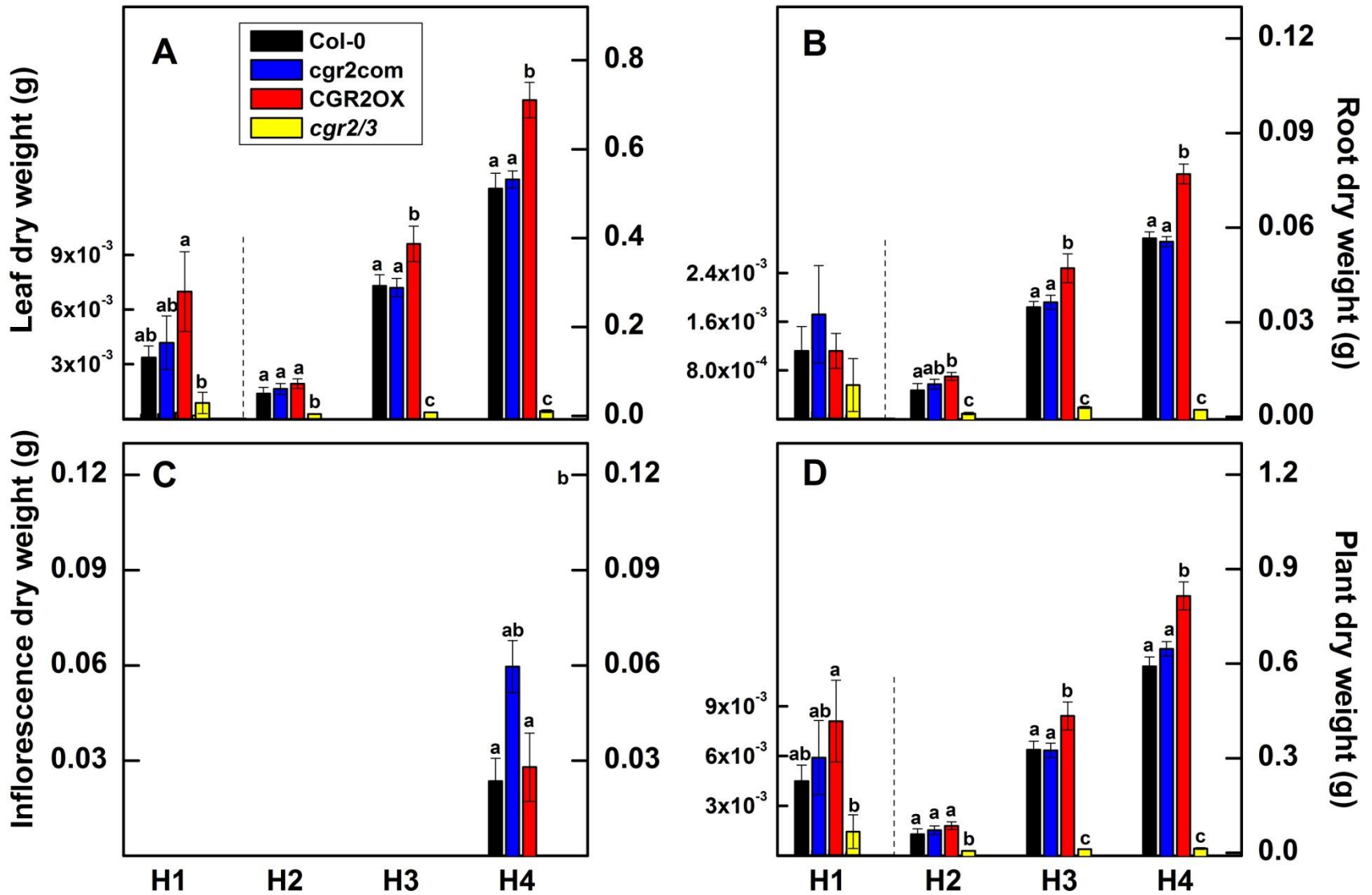


Figure 8. Variations in dry weight overtime in *Arabidopsis* with altered *CGR2* and *CGR3* expression. (A) Leaf, (B) root, (C) inflorescence, and (D) whole plant dry weight at 4 different harvests (H) for Col-0, *cgr2com*, *CGR2OX*, and *cgr2/3* is given. H1, H2, H3 and H4 correspond to 29, 49, 63 and 82 DAS, respectively. Values represent the mean \pm SE and n = 5 plants per line. Statistical differences at $\alpha = 0.05$ are indicated by different letters. All rights reserved.

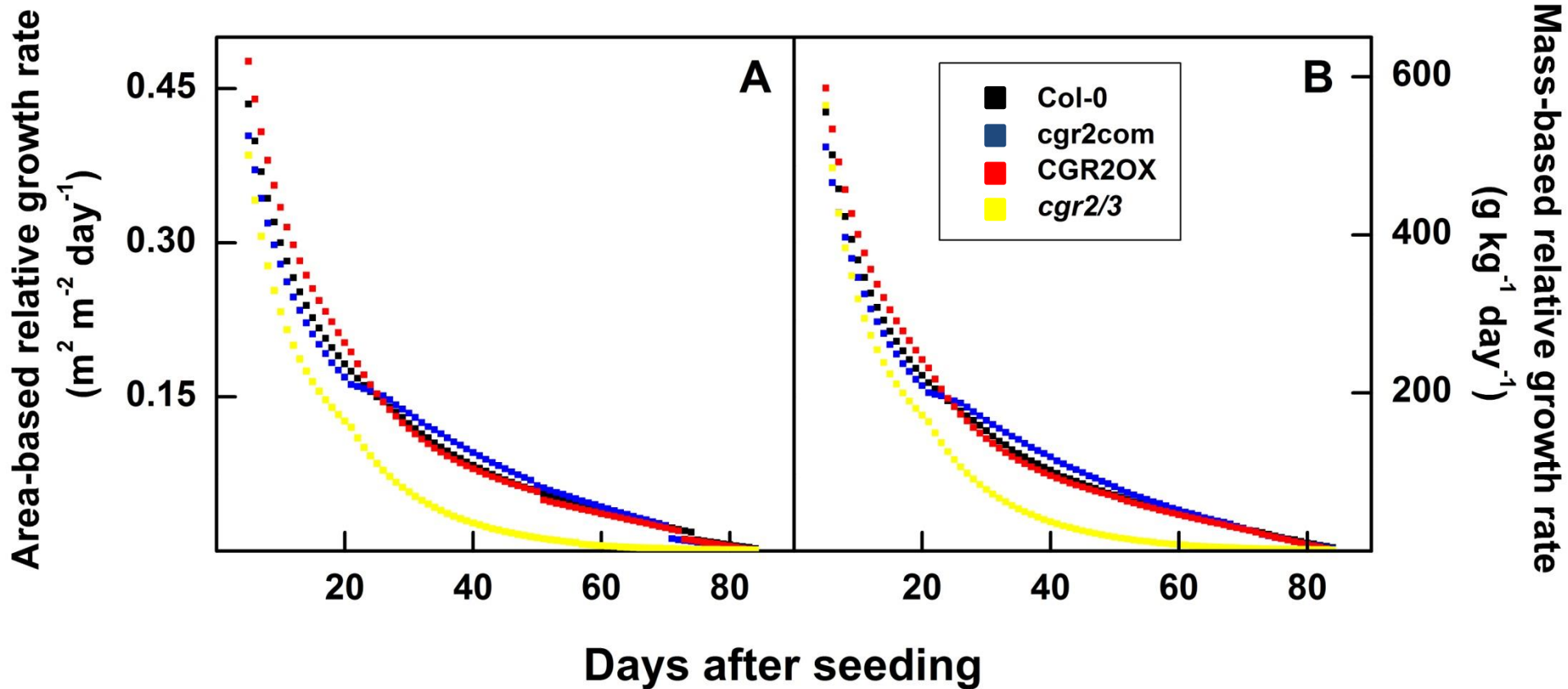


Figure 9. Modeled relative growth rates overtime in *Arabidopsis* with altered *CGR2* and *CGR3* expression. (A) Area-based relative growth rates and (B) mass-based relative growth rates simulated from day 5-84 using the *Arabidopsis* Leaf Area Growth Model fitted with data obtained from Col-0, *cgr2com*, CGR2OX, and *cgr2/3* is presented.

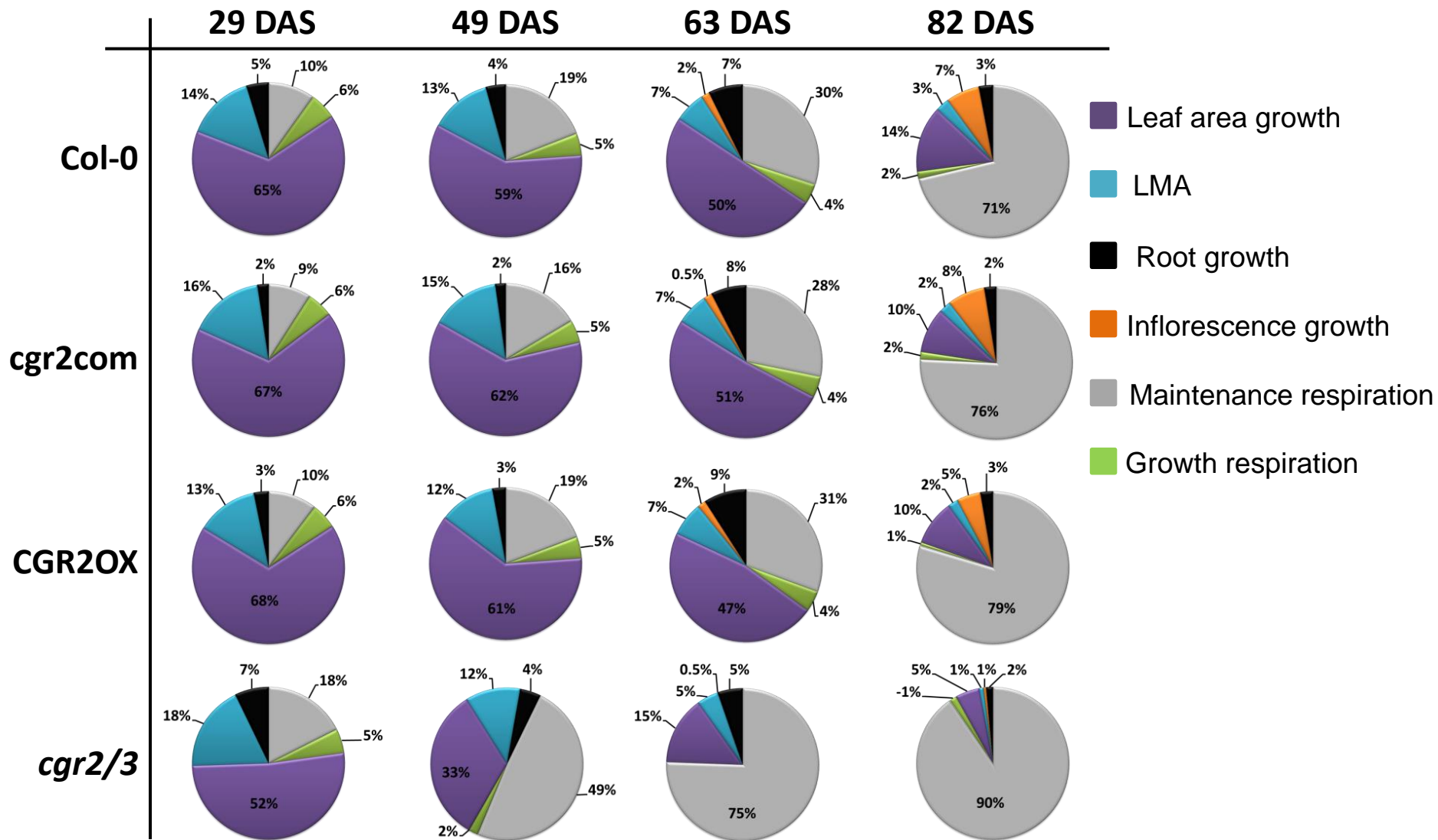
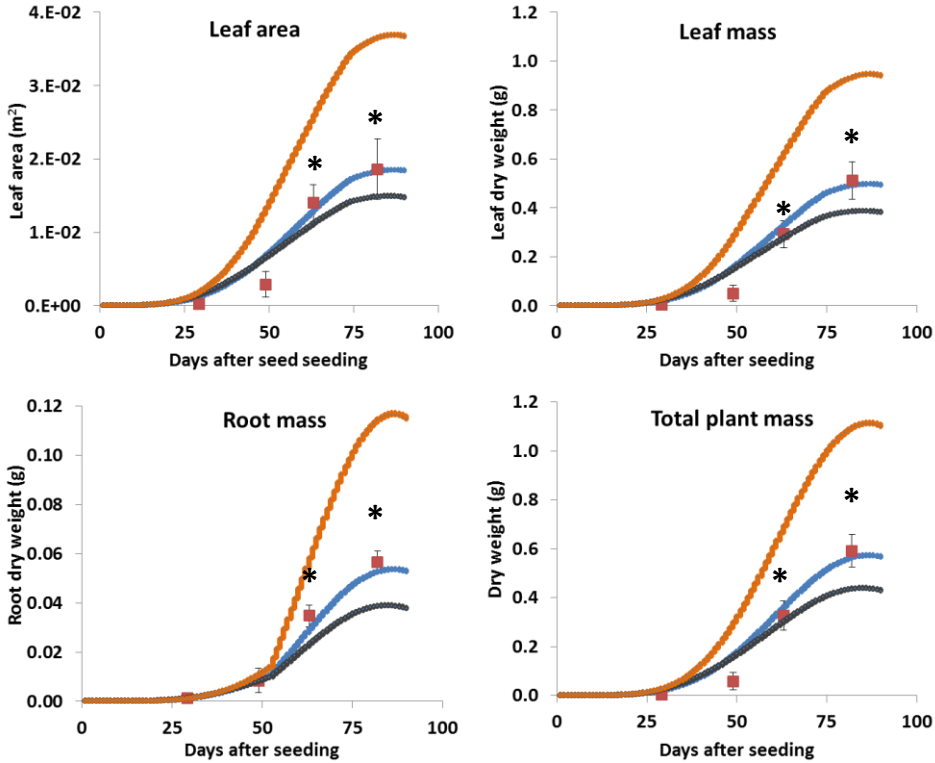
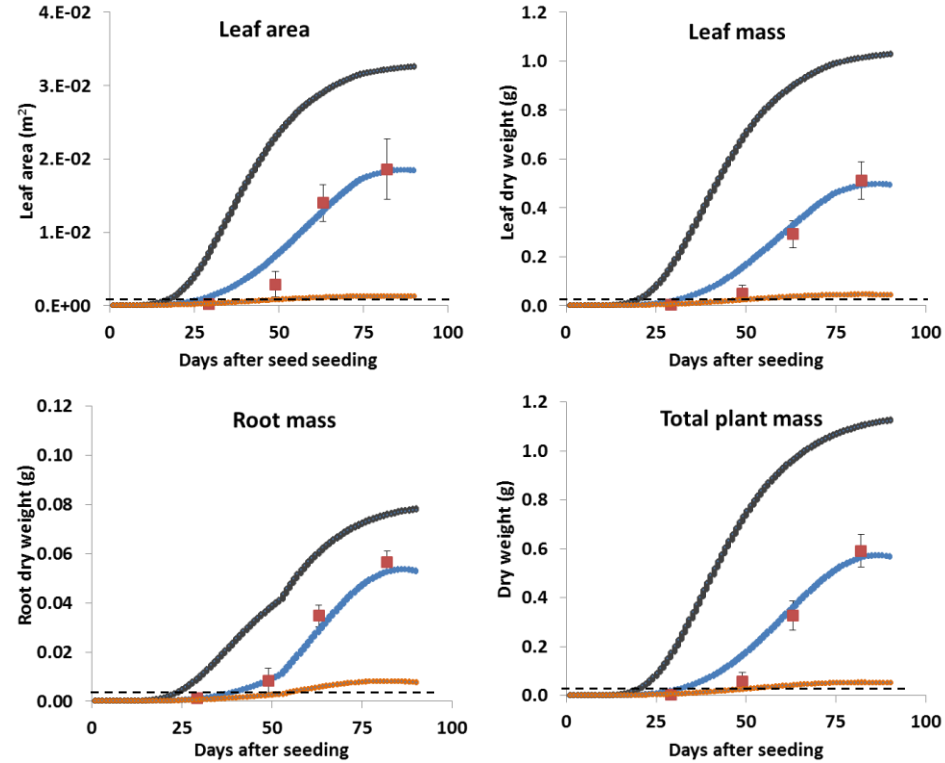


Figure 10. Modeled C partitioning to growth and respiration in *Arabidopsis* with altered *CGR2* and *CGR3* expression. C partitioned to support growth in terms of leaf area and LMA, and inflorescence growth, root growth, and maintenance and growth respiration is presented as percentages of the daily available C at 29, 49, 63 and 82 DAS. Data was derived from the *Arabidopsis* Leaf Area Growth Model fitted with data obtained from Col-0, *cgr2com*, *CGR2OX*, and *cgr2/3*.

A

Modeled effects on growth when either photosynthetic rates or partitioning coefficients for Col-0 is replaced by that of CGR2OX

B

Modeled effects on growth when either photosynthetic rates or partitioning coefficients for Col-0 is replaced by that of *cgr2/3*

Figure 11. Comparison of the effects of altered area-based photosynthesis and C partitioning coefficients on plant growth in *Arabidopsis* with altered *CGR2* and *CGR3* expression. Modeled effects on leaf area and leaf, root, and plant dry weights when either photosynthetic rates or partitioning coefficients spanning the entire growth cycle for Col-0 is replaced by that of (A) *CGR2OX* and (B) *cgr2/3* are presented. In (A) and (B), blue lines represent modeled growth for Col-0 and red squares represent measured data points (mean \pm SD) for Col-0 at 29, 49, 63, and 82 DAS. Grey lines represent modeled data for Col-0 when its area-based photosynthesis rates are replaced by that of either *CGR2OX* (A) or *cgr2/3* (B). Orange lines represent modeled data for Col-0 when its partitioning coefficients (Table 1) are replaced by that of either *CGR2OX* (A) or *cgr2/3* (B) without making any changes to area-based photosynthesis rates of Col-0. In (A), asterisks represent measured data for *CGR2OX* at 63 and 82 DAS. In (B), the dotted line indicates the upper limit of measured data for *cgr2/3*.

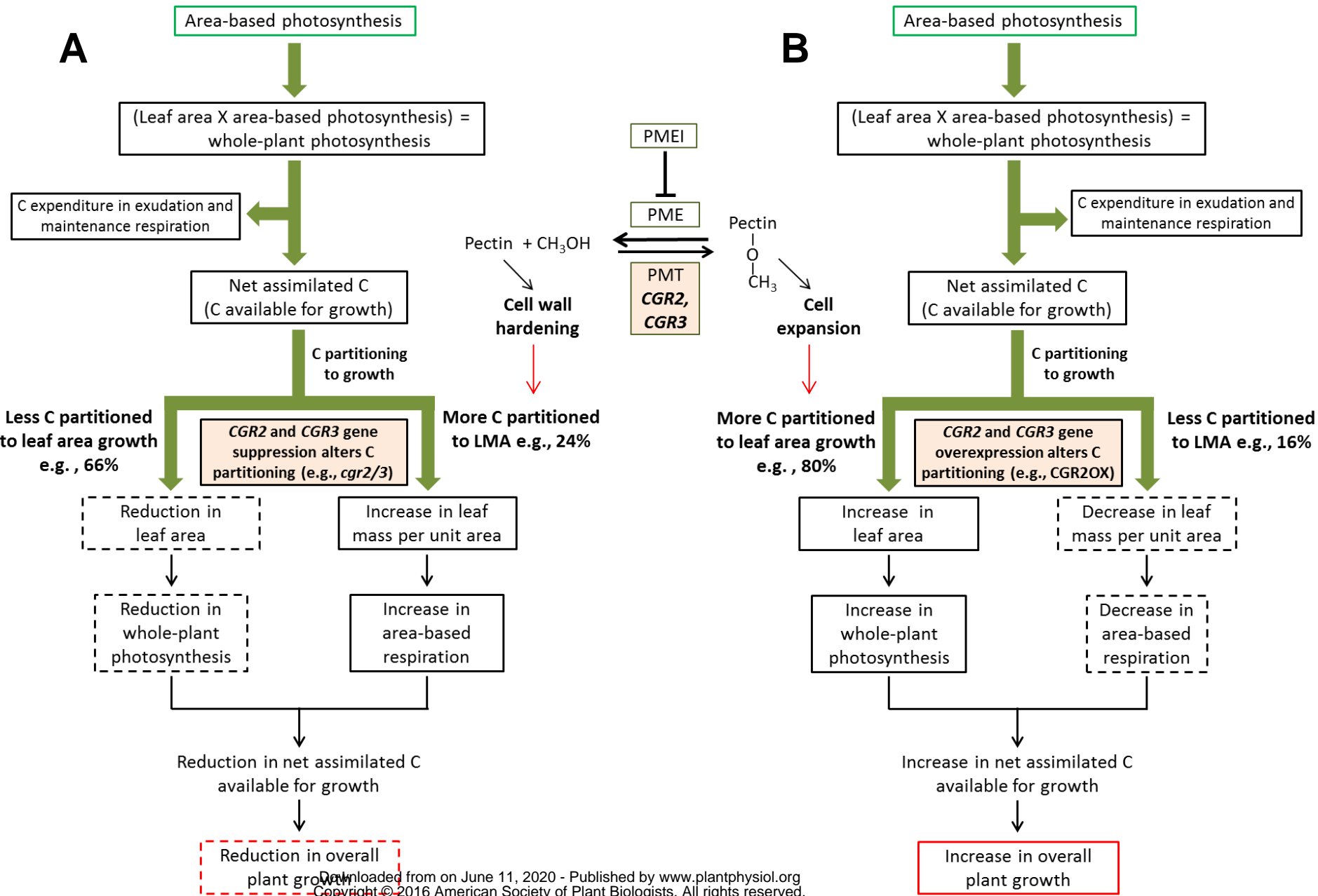


Figure 12. *CGR2* and *CGR3* mediated pectin methylesterification regulates the relationship between photosynthesis and plant growth. A schematic diagram outlining how (A) suppression or (B) overexpression of *CGR2* and *CGR3* gene expression affects the relationship between photosynthesis and plant growth in *Arabidopsis thaliana* is presented. Suppression of *CGR2* and *CGR3* reduces the degree of pectin methylation which leads to an increase in cell to cell adhesion, cation mediated cross linking of galacturonic acid and consequent hardening of cell walls. *CGR2* overexpression increases the degree of pectin methylation which allows cell expansion through reduced cell to cell adhesion and cation mediated cross-linking. We propose that pectin methyltransferase enzyme, through its ability to directly alter cell expansion, determines the amount of C partitioned to leaf area growth vs. leaf thickening. For example, while more C is partitioned to growth in terms of leaf mass per unit area (LMA) in the *CGR2* and *CGR3* double knockout mutant, in the *CGR2* overexpression line more C is partitioned to leaf area growth. An increase in LMA leads to enhanced area-based respiration and a reduction in leaf area contribute to a reduction in whole plant photosynthesis. Collectively, this results in a reduction in C available for growth and consequently a decrease in overall plant growth; an opposite trend is seen in *CGR2OX*. Thus, *CGR2* and *CGR3* through their ability to alter the degree of methylated pectin in the cell wall of the mesophyll cells, determines how photosynthate is utilized to grow the plant. In other words, *CGR2* and *CGR3* mediated pectin methylesterification affects the relationship between photosynthesis and plant growth by regulating the proportions of C that is partitioned to leaf area growth and LMA. Final overall growth mainly depends on the expression patterns of *CGR2* and *CGR3* and how much C is partitioned to area growth and LMA and not on area-based photosynthesis. Abbreviations: PME – pectin methylesterase, PMEI – PME inhibitor, PMT – pectin methyltransferase. CH₃OH is methanol.

Parsed Citations

Amthor JS (1984) The role of maintenance respiration in plant growth. Plant Cell Environ 7: 561-569

Pubmed: [Author and Title](#)

CrossRef: [Author and Title](#)

Google Scholar: [Author Only](#) [Title Only](#) [Author and Title](#)

Burton RA, Gibeaut DM, Bacic A, Findlay K, Roberts K, Hamilton A, Baulcombe DC, Fincher GB (2000) Virus-induced silencing of a plant cellulose synthase gene. Plant Cell 12: 691-705

Pubmed: [Author and Title](#)

CrossRef: [Author and Title](#)

Google Scholar: [Author Only](#) [Title Only](#) [Author and Title](#)

Caffall KH, Mohnen D (2009) The structure, function, and biosynthesis of plant cell wall pectic polysaccharides. Carbohydr Res 344: 1879-1900

Pubmed: [Author and Title](#)

CrossRef: [Author and Title](#)

Google Scholar: [Author Only](#) [Title Only](#) [Author and Title](#)

Cunningham SA, Summerhayes B, Westoby M (1999) Evolutionary divergences in leaf structure and chemistry, comparing rainfall and soil nutrient gradients. Ecol Monogr 69: 569-588

Pubmed: [Author and Title](#)

CrossRef: [Author and Title](#)

Google Scholar: [Author Only](#) [Title Only](#) [Author and Title](#)

De Vries FWTP, Brunsting AHM, Van Laar HH (1974) Products, requirements and efficiency of biosynthesis a quantitative approach. J Theor Biol 45: 339-377

Pubmed: [Author and Title](#)

CrossRef: [Author and Title](#)

Google Scholar: [Author Only](#) [Title Only](#) [Author and Title](#)

Evans JR, Caemmerer Sv, Setchell BA, Hudson GS (1994) The relationship between CO₂ transfer conductance and leaf anatomy in transgenic tobacco with a reduced content of rubisco. Aust J Plant Physiol 21: 475-495

Pubmed: [Author and Title](#)

CrossRef: [Author and Title](#)

Google Scholar: [Author Only](#) [Title Only](#) [Author and Title](#)

Farquhar G, Ehleringer J, Hubick K (1989) Carbon isotope discrimination and photosynthesis. Annu Rev Plant Physiol Plant Mol Biol 40: 503-537

Pubmed: [Author and Title](#)

CrossRef: [Author and Title](#)

Google Scholar: [Author Only](#) [Title Only](#) [Author and Title](#)

Farquhar G, O'Leary M, Berry J (1982) On the relationship between carbon isotope discrimination and the intercellular carbon dioxide concentration in leaves. Funct Plant Biol 9: 121-137

Pubmed: [Author and Title](#)

CrossRef: [Author and Title](#)

Google Scholar: [Author Only](#) [Title Only](#) [Author and Title](#)

Galmés J, Ochogavía JM, Gago J, Roldán EJ, Cifre J, Conesa MÀ (2013) Leaf responses to drought stress in mediterranean accessions of *Solanum lycopersicum*: anatomical adaptations in relation to gas exchange parameters. Plant Cell Environ 36: 920-935

Pubmed: [Author and Title](#)

CrossRef: [Author and Title](#)

Google Scholar: [Author Only](#) [Title Only](#) [Author and Title](#)

Heldt H-W, Piechulla B (2010) Plant Biochemistry, Ed 4. Academic Press, London, UK

Pubmed: [Author and Title](#)

CrossRef: [Author and Title](#)

Google Scholar: [Author Only](#) [Title Only](#) [Author and Title](#)

Honda H, Fisher JB (1978) Tree branch angle: maximizing effective leaf area. Science 199: 888-890

Pubmed: [Author and Title](#)

CrossRef: [Author and Title](#)

Google Scholar: [Author Only](#) [Title Only](#) [Author and Title](#)

Kim HS, Delaney TP (2002) Over-expression of TGA5, which encodes a bZIP transcription factor that interacts with NIM1/NPR1, confers SAR-independent resistance in *Arabidopsis thaliana* to *Peronospora parasitica*. Plant J 32: 151-163

Pubmed: [Author and Title](#)

CrossRef: [Author and Title](#)

Google Scholar: [Author Only](#) [Title Only](#) [Author and Title](#)

Kim S-J, Held MA, Zemelis S, Wilkerson C, Brandizzi F (2015) CGR2 and CGR3 have critical overlapping roles in pectin methylesterification and plant growth in *Arabidopsis thaliana*. Plant J 82: 208-220

Pubmed: [Author and Title](#)

CrossRef: [Author and Title](#)

Google Scholar: [Author Only](#) [Title Only](#) [Author and Title](#)

Lambers H, Chapin F, Pons T (2008) Plant Physiological Ecology, Ed 2. Springer., NewYork, NY

Pubmed: [Author and Title](#)

Downloaded from on June 11, 2020 - Published by www.plantphysiol.org
Copyright © 2016 American Society of Plant Biologists. All rights reserved.

CrossRef: [Author and Title](#)
Google Scholar: [Author Only](#) [Title Only](#) [Author and Title](#)

Lionetti V, Raiola A, Camardella L, Giovane A, Obel N, Pauly M, Favaron F, Cervone F, Bellincampi D (2007) Overexpression of pectin methylesterase inhibitors in Arabidopsis restricts fungal infection by Botrytis cinerea. Plant Physiol 143: 1871-1880

Pubmed: [Author and Title](#)
CrossRef: [Author and Title](#)
Google Scholar: [Author Only](#) [Title Only](#) [Author and Title](#)

Liu YB, Lu SM, Zhang JF, Liu S, Lu YT (2007) A xyloglucan endotransglucosylase/hydrolase involves in growth of primary root and alters the deposition of cellulose in Arabidopsis. Planta 226: 1547-1560

Pubmed: [Author and Title](#)
CrossRef: [Author and Title](#)
Google Scholar: [Author Only](#) [Title Only](#) [Author and Title](#)

Mariko S (1988) Maintenance and constructive respiration in various organs of Helianthus annuus L. and Zinnia elegans L. Bot Mag 101: 73

Pubmed: [Author and Title](#)
CrossRef: [Author and Title](#)
Google Scholar: [Author Only](#) [Title Only](#) [Author and Title](#)

Mitchell KA, Bolstad PV, Vose JM (1999) Interspecific and environmentally induced variation in foliar dark respiration among eighteen southeastern deciduous tree species. Tree Physiol 19: 861-870

Pubmed: [Author and Title](#)
CrossRef: [Author and Title](#)
Google Scholar: [Author Only](#) [Title Only](#) [Author and Title](#)

Miura K, Hasegawa PM (2010) Sumoylation and other ubiquitin-like post-translational modifications in plants. Trends Cell Biol 20: 223-232

Pubmed: [Author and Title](#)
CrossRef: [Author and Title](#)
Google Scholar: [Author Only](#) [Title Only](#) [Author and Title](#)

Pilling J, Willmitzer L, Bucking H, Fisahn J (2004) Inhibition of a ubiquitously expressed pectin methyl esterase in Solanum tuberosum L. affects plant growth, leaf growth polarity, and ion partitioning. Planta 219: 32-40

Pubmed: [Author and Title](#)
CrossRef: [Author and Title](#)
Google Scholar: [Author Only](#) [Title Only](#) [Author and Title](#)

Poorter H, Niinemets U, Poorter L, Wright IJ, Villar R (2009) Causes and consequences of variation in leaf mass per area (LMA): a meta-analysis. New Phytol 182: 565-588

Pubmed: [Author and Title](#)
CrossRef: [Author and Title](#)
Google Scholar: [Author Only](#) [Title Only](#) [Author and Title](#)

Shipley B (2002) Trade-offs between net assimilation rate and specific leaf area in determining relative growth rate: relationship with daily irradiance. Funct Ecol 16: 682-689

Pubmed: [Author and Title](#)
CrossRef: [Author and Title](#)
Google Scholar: [Author Only](#) [Title Only](#) [Author and Title](#)

Terashima I, Hanba YT, Tazoe Y, Vyas P, Yano S (2006) Irradiance and phenotype: comparative eco-development of sun and shade leaves in relation to photosynthetic CO₂ diffusion. J Exp Bot 57: 343-354

Pubmed: [Author and Title](#)
CrossRef: [Author and Title](#)
Google Scholar: [Author Only](#) [Title Only](#) [Author and Title](#)

Thomas RB, Reid CD, Yberna R, Strain BR (1993) Growth and maintenance components of leaf respiration of cotton grown in elevated carbon dioxide partial pressure. Plant Cell Environ 16: 539-546

Pubmed: [Author and Title](#)
CrossRef: [Author and Title](#)
Google Scholar: [Author Only](#) [Title Only](#) [Author and Title](#)

Tsuge T, Tsukaya H, Uchimiya H (1996) Two independent and polarized processes of cell elongation regulate leaf blade expansion in Arabidopsis thaliana (L.) Heynh. Development 122: 1589-1600

Pubmed: [Author and Title](#)
CrossRef: [Author and Title](#)
Google Scholar: [Author Only](#) [Title Only](#) [Author and Title](#)

Villar R, Ruiz-Robledo J, Uberta JL, Poorter H (2013) Exploring variation in leaf mass per area (LMA) from leaf to cell: an anatomical analysis of 26 woody species. Am J Bot 100: 1969-1980

Pubmed: [Author and Title](#)
CrossRef: [Author and Title](#)
Google Scholar: [Author Only](#) [Title Only](#) [Author and Title](#)

Weraduwege SM, Chen J, Anozie FC, Morales A, Weise SE, Sharkey TD (2015) The relationship between leaf area growth and biomass accumulation in Arabidopsis thaliana. Front Plant Sci 6

Pubmed: [Author and Title](#)
CrossRef: [Author and Title](#)
Google Scholar: [Author Only](#) [Title Only](#) [Author and Title](#)

Witkowski ETF, Lamont B (1991) Leaf specific mass confounds leaf density and thickness. *Oecologia* 88: 486-493

Pubmed: [Author and Title](#)

CrossRef: [Author and Title](#)

Google Scholar: [Author Only](#) [Title Only](#) [Author and Title](#)

Wolf S, Mouille G, Pelloux J (2009) Homogalacturonan methyl-esterification and plant development. *Molecular Plant* 2: 851-860

Pubmed: [Author and Title](#)

CrossRef: [Author and Title](#)

Google Scholar: [Author Only](#) [Title Only](#) [Author and Title](#)

Xiao C, Anderson CT (2013) Roles of pectin in biomass yield and processing for biofuels. *Front Plant Sci* 4

Pubmed: [Author and Title](#)

CrossRef: [Author and Title](#)

Google Scholar: [Author Only](#) [Title Only](#) [Author and Title](#)